
iDSE: Navigating Design Space Exploration in High-Level Synthesis Using LLMs

Runkai Li*
Southeast University

Jia Xiong*
Southeast University

Xi Wang†
Southeast University

Abstract

High-Level Synthesis (HLS) serves as an agile hardware development tool that streamlines the circuit design by abstracting the register transfer level into behavioral descriptions, while allowing designers to customize the generated microarchitectures through optimization directives. However, the combinatorial explosion of possible directive configurations yields an intractable design space. Traditional design space exploration (DSE) methods, despite adopting heuristics or constructing predictive models to accelerate Pareto-optimal design acquisition, still suffer from prohibitive exploration costs and suboptimal results. Addressing these concerns, we introduce iDSE, the first LLM-aided DSE framework that leverages HLS design quality perception to effectively navigate the design space. iDSE intelligently prunes the design space to guide LLMs in calibrating representative initial sampling designs, expediting convergence toward the Pareto front. By exploiting the convergent and divergent thinking patterns inherent in LLMs for hardware optimization, iDSE achieves multi-path refinement of the design quality and diversity. Extensive experiments demonstrate that iDSE outperforms heuristic-based DSE methods by $5.1 \times \sim 16.6 \times$ in proximity to the reference Pareto front, matching NSGA-II with only 4.6% of the explored designs. Our work demonstrates the transformative potential of LLMs in scalable and efficient HLS design optimization, offering new insights into multiobjective optimization challenges.

1 Introduction

Transistor scaling has driven exponential performance improvements in modern circuits, yet it remains incapable of accommodating the escalating computational demands in fields such as neural networks [1–4], computer vision [5, 6], robotics [7, 8], and genome sequence analysis [9–12]. The development of domain-specific accelerators (DSAs) tailored to specific workloads has shown notable growth [13, 14]. However, the protracted chip design and verification cycles impede the swift iteration of DSAs required to keep pace with the rapidly evolving dedicated application requirements. High-Level Synthesis (HLS) abstracts hardware description languages (HDL) into behavioral representation, accelerating FPGA-based prototyping with comparable circuit performance and improved hardware development efficiency [15, 16]. Furthermore, most vendor HLS tools incorporate optimization directives to customize microarchitectures, synthesized from high-level programming languages, to align design requirements with quality of results (QoR). However, the extensive permutations of directive configurations constitute an expansive design space, rendering the identification of Pareto-optimal designs challenging and expertise-intensive, as illustrated in Figure 1.

To capitalize the reconfigurability and scalability advantages of HLS and advance hardware optimization, recent research has focused on automated and efficient design space exploration (DSE) methods

*Equal contribution.

†Corresponding author: Xi Wang (xi.wang@seu.edu.cn).

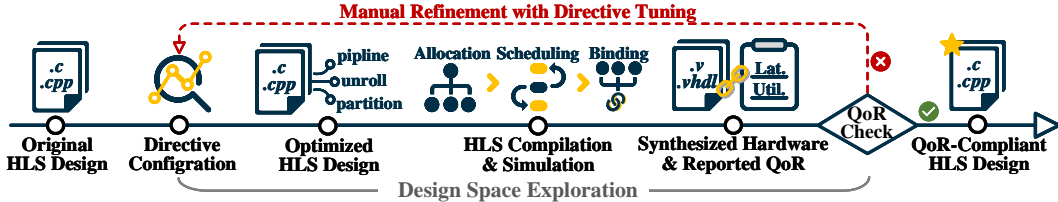


Figure 1: Time-consuming manual directive configuration tuning based on QoR reported in HLS.

aimed at reducing manual intervention. However, the extensive combination of directives exponentially expands the design space. Furthermore, the time-consuming performance evaluation required by HLS tools renders exhaustive traversal impractical. Traditional DSE methods typically treat HLS as a black-box optimization problem, relying heavily on heuristics that necessitate multiple iterations to approximate Pareto-optimal solutions. This approach often results in prolonged exploration periods and inadequate coverage of optimal designs [17–22]. In response, machine learning (ML) and deep learning (DL) techniques have revisited DSE by leveraging predictive models to surrogate expensive HLS evaluations. These approaches significantly improve efficiency by enabling the evaluation of substantially more designs [23–31]. However, model-based methods typically involve significant training overhead and exhibit limited generalization across unseen workloads, HLS environments, or varied hardware constraints, potentially compromising the optimality of explored designs.

Recently, Large Language Models (LLMs) have attracted considerable attention for their exceptional proficiency in natural language processing and code generation. However, their effectiveness in specialized applications is often hampered by limited domain-specific data. Previous efforts have harnessed the code generation and debugging capabilities of LLMs to streamline chip design and verification workflows, highlighting their potential to improve efficiency within electronic design automation (EDA) [32–36]. Despite these advancements, existing approaches have not sufficiently exploited LLMs to achieve a high degree of hardware optimization for high-quality circuits required by emerging applications. Recent research has demonstrated considerable promise in employing LLMs for gradient-free black-box optimization tasks [37–41]. Such approaches leverage the natural language reasoning capabilities of LLMs, enabling iterative and informed exploration of optimization trajectories through linguistic prompting. HLS abstracts hardware designs to the algorithmic level while ensuring functional equivalence, providing an opportunity to empower hardware optimization by directing LLMs towards the design structure, thus reducing hardware specification semantics. Furthermore, leveraging the inherent domain expertise and reasoning capabilities in LLMs, it becomes feasible to efficiently allocate operational parallelism in HLS-generated hardware.

Building on this insight, we propose **iDSE**, a novel LLM-navigated DSE framework that reduces time costs and expertise barriers for HLS design optimization. This framework automates the end-to-end process by extracting HLS design features and pruning invalid designs, thus effectively distilling the design space. Furthermore, iDSE incorporates a warm-start mechanism, which initializes exploration with representative seed designs to accelerate convergence to the Pareto front. By employing operators inspired by evolutionary algorithms to spawn refined design candidates, iDSE capitalizes on prior knowledge to analyze design bottlenecks, identify optimization opportunities and refine designs. Quantitative metrics highlight that our framework shapes a broader and more concave Pareto front, providing a new perspective for promoting the customization of DSAs.

The main contributions of this paper are as follows:

- We introduce **iDSE**, the **first** end-to-end design space exploration framework integrating optimization trajectory awareness with prior expertise injection. This presents a compelling direction for conquering the intricate challenges of automated hardware optimization.
- We propose a scalable **Feature-Driven Pruning** approach to significantly expedite the DSE iterations by constructing a compact yet expressive HLS design space.
- We reimagine DSE initialization through the LLM-guided **Seed Directive Generation** methodology. This approach enables warm-starts that rapidly converge toward comprehensive and concave Pareto front profiling by improving the quality and diversity of the initial sampling designs.
- We introduce a novel **QoR-Aware Adaptive Optimization** system that exploits the convergent and divergent thinking capabilities of LLMs to navigate multi-path HLS design optimization. By perceiving QoR feedback, our system transcends existing bottlenecks and escapes local optima.

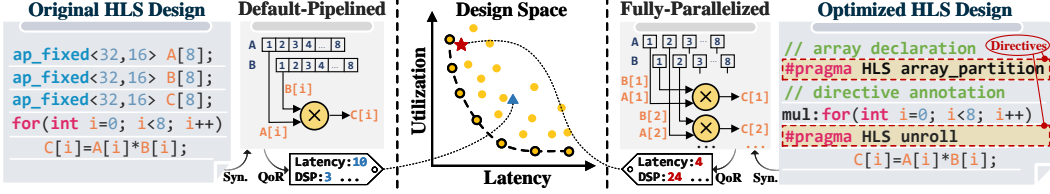


Figure 2: Example of customizing synthesized hardware with HLS optimization directives. **Left:** Default loop *read-compute-write* pipelining structure without specifying any directives. **Middle:** QoR mapping across the design space. **Right:** Fully parallelized memory access and loop operations.

- Our extensive experiments across diverse HLS benchmarks demonstrate **5.1×**–**~16.6×** improvement in explored Pareto front quality over heuristic-based DSE methods, with up to **25.1×** higher exploration efficiency. This work reveals the unique potential of LLM-aided hardware optimization.

2 Background & Related Work

High-Level Synthesis Design Space Exploration. HLS employs optimization directives to transform high-level description languages (C/C++/System C) into specific microarchitectures through hardware resource allocation, and operation scheduling/binding. While designers typically prioritize Pareto-optimal solutions that satisfy certain constraints, the exponentially growing design space compiled by the Cartesian product of directives renders brute-force traversal computationally infeasible, particularly given the time-consuming quality of results (QoR) evaluation for each configuration. Figure 2 illustrates a toy example for implementing and optimizing a vector Hadamard product in HLS. Although this HLS design contains only one loop and three arrays, considering the loop and memory access parallelization directives supported in this paper, where the factors for loop unrolling and memory partitioning are divisors of loop and array boundaries, we still obtain **1.58M valid** designs composed of various combinations and parameters of directives. Exhaustively evaluating all designs would require approximately **3 years**, assuming only one minute per configuration evaluation.

Meta-heuristic [17–20, 42] and dedicated heuristic [22, 43–45] DSE methods treat the HLS tool as a black box, leveraging hardware optimization characteristics to efficiently approximate Pareto-optimal solutions. While exhaustive searches are avoided, these methods still necessitate multiple invocations of the HLS tool to guide optimization trajectories. Moreover, their effectiveness remains constrained by initial sampling quality, limiting exploration within a confined design space under restricted search budgets. The introduction of ML and DL methods has driven the construction of analysis models for QoR prediction [27, 28, 46, 47]. By providing surrogate models for HLS tool evaluations, these methods enable performance and resource utilization predictions for the synthesized hardware. Graph neural networks (GNNs) embed program nodes and directive configurations have notably improved prediction accuracy [24–26, 48]. However, ML/DL-based approaches demand substantial training and deployment costs, exhibit limited generalization across different applications and versions of vendor HLS tools. Additionally, these methods often focus on optimizing a single performance metric, thereby overlooking the full spectrum of optimization requirements.

LLM-Aided Hardware Design. Integration of LLMs has catalyzed the evolution of EDA tools [32–35, 49–58]. However, current efforts struggle to keep pace with the rapidly evolving application requirements, and achieving modern high-performance computing architectures remains challenging, necessitating breakthroughs in LLM-aided hardware optimization. Previous research on LLMs applying to HLS has examined their capability to insert directives into source code, utilizing knowledge-augmented technology to bridge the expertise gap in HLS [59–63]. However, the results have been underwhelming, with code transformations frequently introducing synthesis errors. Furthermore, existing studies primarily target performance-optimal designs, identifying HLS designs across the Pareto front to accommodate diverse optimization preferences remains nascent [64, 65]. This research gap obscures the practical implementation of LLMs in hardware optimization contexts.

Machine Learning in Multiobjective Optimization. Different from conventional multiobjective optimization methods [66–73], recent research has demonstrated significant improvements in heuristic optimization [41, 74–78] and neural architecture search [79–84] by embedding LLMs into evolutionary algorithms (EA). This approach outperforms manual tuning and traditional automated approaches, highlighting the promise of LLM-driven multiobjective optimization. Some research

has employed LLM-enhanced EA operators in conjunction with GNN-based predictive models for DSE [85]. However, substituting actual evaluation with regression models inevitably compromises performance. Meanwhile, existing LLM implementations of EA often yield suboptimal results due to inadequate reflection on optimization trajectories and a lack of task-specific guidance for DSE.

3 Preliminary & Problem Formulation

Balancing computation and memory access parallelism under hardware resource constraints to achieve satisfactory circuit performance is a delicate process. Since performance improvements and resource consumption are often contradictory, DSE constitutes a multiobjective optimization problem. We focus on two primary objectives in DSE: **execution latency** and **resource utilization**. For an HLS design $\lambda(\varphi)$, φ represents the inserted optimization directives, this work emphasizes three directives, PIPELINE (\mathcal{LP}), UNROLL (\mathcal{LU}), ARRAY_PARTITION (\mathcal{AP}), which control loop execution and memory access parallelism. Define φ as a feature vector $\varphi = [\mathcal{LP}_i, \mathcal{LU}_j, \mathcal{AP}_{k,d}]$, where \mathcal{LP}_i is a boolean used to enable loop i pipelining, \mathcal{LU}_j is the unroll factor for loop j , and $\mathcal{AP}_{k,d}$ is the partition type and factor for array k along dimension d . Under vendor HLS tool \mathcal{H} , we analyze the QoR of the explored design using latency $Lat(\mathcal{H}, \lambda(\varphi))$ and resource utilization $Util(\mathcal{H}, \lambda(\varphi))$.

Definition 1 (Multiobjective Optimization of DSE). The multiobjective DSE task is defined as:

$$\lambda(\varphi^*) = \arg \min_{\varphi \in \Phi \subset \mathbb{Z}^n} [Lat(\mathcal{H}, \lambda(\varphi)), Util(\mathcal{H}, \lambda(\varphi))] \quad (1)$$

We aim to optimize both objectives without significantly compromising either. The goal of DSE is to rapidly and accurately search the design space Φ for Pareto-optimal designs.

Definition 2 (Pareto-Optimal Designs). The explored designs $\lambda(\varphi^*)$ and $\lambda(\varphi^a)$ if:

$$Lat(\mathcal{H}, \lambda(\varphi^*)) \leq Lat(\mathcal{H}, \lambda(\varphi^a)), \quad Util(\mathcal{H}, \lambda(\varphi^*)) \leq Util(\mathcal{H}, \lambda(\varphi^a)) \quad (2)$$

We call it $\lambda(\varphi^*)$ dominates $\lambda(\varphi^a)$. If no other $\varphi \in \Phi$ dominates $\lambda(\varphi^*)$, then $\lambda(\varphi^*)$ is called a Pareto-optimal design. All such designs form the Pareto front.

Definition 3 (Effectiveness of DSE). We employ the average distance to reference set (ADRS) metric to quantify the gap $d(\cdot)$ between an explored Pareto front P_E and a reference Pareto front P_R [86]:

$$ADRS(P_E, P_R) = \frac{1}{|P_R|} \sum_{\lambda(\varphi^\gamma) \in P_R} \min_{\lambda(\varphi^\omega) \in P_E} d(\lambda(\varphi^\gamma), \lambda(\varphi^\omega)) \quad (3)$$

A small ADRS indicates that the explored designs more effectively approximate the entire reference Pareto front. Achieving a small ADRS within constrained search budgets demonstrates the performance and efficiency of the proposed DSE method.

4 iDSE Design & Philosophy

Our framework, **iDSE**, automates the exploration of design spaces to optimize HLS designs with LLM as the backbone, effectively identifying Pareto-optimal designs while balancing competing objectives. The workflow of iDSE, depicted in Figure 3, unfolds in three distinct stages:

1) Preprocessing. iDSE first extracts a unified design space from the provided HLS design and employs specific pruning strategies to eliminate invalid directive configurations that may result in ineffective or inefficient synthesis. This step defines a feasible domain and narrows the parameter ranges to be searched, thereby improving the efficiency of approximating the Pareto front.

2) Warm-Start. iDSE then leverages the LLM to reproduce the learned insights to identify directive configurations with optimization potential from the expansive design space, providing high-quality and discrete sampling designs to warm-start subsequent optimization.

3) Adaptive Optimization. To further approximate the Pareto front, iDSE performs a bottleneck analysis on initial sampling designs, guided by empirical optimization knowledge, which prompts LLM to conduct oriented reasoning for localized design refinement. Furthermore, iDSE exploits the divergent thinking of LLMs to escape limitations of existing optimization strategies and propose novel optimization directions, thus expanding the exploration scope and improving design diversity.

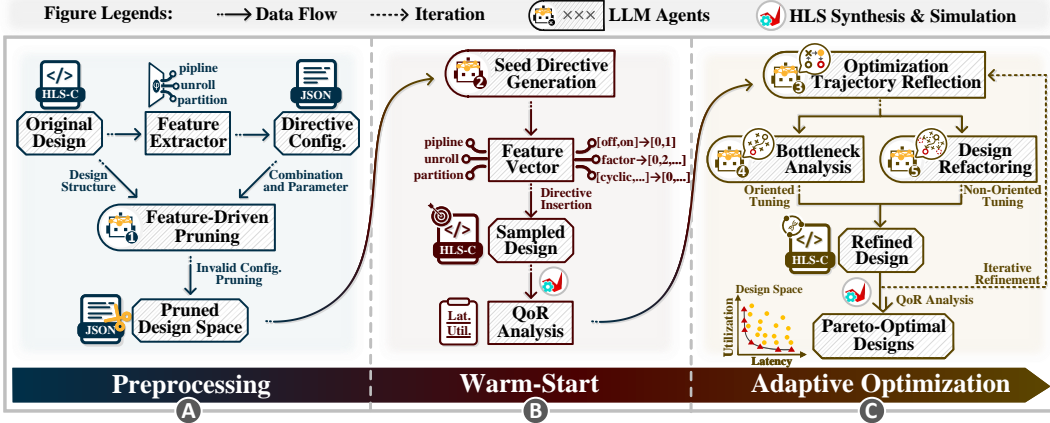


Figure 3: iDSE Workflow

4.1 Preprocessing: Directive Configuration Extraction and Design Space Pruning

The allocation of loop and memory access parallelism constitutes a critical bottleneck in hardware optimization, significantly affecting both performance and resource utilization of synthesized hardware designs. *Feature Extractor* parses the design structure to extract key structural metadata (e.g., array dimensions, loop trip counts) that determine feasible parallelism degrees for optimization directive combinations and parameters. However, for large design footprints, this may introduce aggressive parallelism that makes the generated optimization strategy infeasible.

Building upon these extracted features, we propose the **Feature-Driven Pruning** approach, which eliminates invalid directive configurations that may lead to excessive synthesis time or even failure, thus effectively compressing the design space. This approach prompts the LLM to adopt specific pruning strategies that intelligently identify and remove aggressive parallelism and invalid directive combinations. For example, when examining nested loops with multilayer structures or large inner loop trip counts, judiciously disabling the pipeline option for the outer loop effectively eliminates about half of the invalid designs (pruning strategies are detailed in Appendix A.2). Furthermore, we provide a prompt interface that allows designers to customize their pruning strategies according to specific hardware resource tolerance. Importantly, this method preserves potential Pareto-optimal designs, which would not be extensively missed due to aggressive pruning strategies.

4.2 Warm-Start: LLM-Guided Design Space Exploration Initialization

LLMs can effectively leverage prior knowledge of hardware optimization by emulating the reasoning patterns of seasoned engineers, as similar directives embedded in analogous design structures typically yield comparable QoR [87, 88]. We propose an LLM-guided **Seed Directive Generation** mechanism, which first generates a formatted feature vector of seed directive configuration, and then automatically creates a Tcl script to embed directives into the original HLS design. Meanwhile, this structured directive configuration enables seamless integration with heuristic-based DSE methods.

To ensure high-quality initial sampling designs, we establish specific design principles to guide the LLM in generating directive configurations that can be executed efficiently. This approach prevents the LLM from simply refluxing trivial solutions drawn from its pretraining data (detailed prompt design available in Appendix B). Our initialization strategy begins by defining the sampling task with universal optimization objectives: prioritizing performance, prioritizing resource utilization, and balancing both considerations. By providing the LLM with the structured directive configurations derived from the *preprocessing* stage, we enable it to generate a prescribed number of diverse directive combinations that cover distinct regions of the design space. An automation tool then parses the execution latency and resource utilization metrics from the HLS synthesis report.

4.3 Adaptive Optimization: Multi-Path Directive Tuning with QoR Perception

Current LLMs exhibit performance degradation when handling lengthy contexts and face difficulties when scaling to extensive design spaces. Furthermore, initial sampling alone inadequately captures the mapping between directive allocation strategies and their effectiveness. To address these limitations,

Algorithm 1 Adaptive Optimization for HLS DSE

Input: LLM π_θ , pruned design space Φ , directive configuration φ , HLS design $\lambda(\varphi)$, initial sampling size N_0 , maximum number of generations I_{max} , adaptive population size P_i , vendor HLS tool \mathcal{H} ,
Output: Pareto-optimal designs $\lambda(\varphi^*)$

- 1: Initialize P_0 with $\varphi_{init} \leftarrow \text{WARMSTART}(\pi_\theta, \Phi, N_0, \lambda(\varphi))$ ▷ Section 4.2
- 2: Evaluate quality of results \mathcal{Q} of initial sampling HLS designs $\lambda(\varphi_{init})$ using \mathcal{H}
- 3: **for** $i \leftarrow 0$ to I_{max} **do**
- 4: Label population P_i with rank and crowding distance
- 5: $\lambda(\varphi_{elite}) \leftarrow \text{SEL}(\pi_\theta, \mathcal{Q}, P_i)$ ▷ Optimization trajectory reflection
- 6: $\varphi_c \leftarrow \text{CONVERGENTSEARCH}(\pi_\theta, \Phi, \lambda(\varphi_{elite}))$ ▷ Oriented tuned directive configurations φ_c
- 7: $\varphi_d \leftarrow \text{DIVERGENTSEARCH}(\pi_\theta, \lambda(\varphi_{elite}))$ ▷ Non-oriented tuned directive configurations φ_d
- 8: Embed φ_c and φ_d into original HLS design $\lambda(\varphi)$, evaluate \mathcal{Q} of $\lambda(\varphi_c)$ and $\lambda(\varphi_d)$
- 9: Adaptive population management for P_i
- 10: **end for**
- 11: Select Pareto-optimal designs $\lambda(\varphi^*)$ through non-dominated sorting of all reported \mathcal{Q}
- 12: **return** $\lambda(\varphi^*)$

we propose **QoR-Aware Adaptive Optimization** system that integrates LLM-based optimization trajectory reflection, bottleneck analysis, and design refactoring for HLS design refinement. This system leverages convergent and divergent thinking capabilities of LLMs to expedite Pareto-optimal design acquisition while achieving broader design space coverage. Algorithm 1 details this process.

Optimization Trajectory Reflection. Following the *Warm-Start* phase (lines 1-2), we construct the initial population utilizing the elite individual selection strategy resembling the NSGA-II framework [89], which prioritizes superior designs while maintaining population diversity, ensuring both coverage and uniform distribution along the explored Pareto front (line 4). For labeled designs and their QoR, we prompt the LLM to perform reflection on the optimization trajectory, thus facilitating the sensible selection of directive configurations with optimization potential. Subsequently, a lightweight analysis examines the selected designs for data dependencies that potentially block pipeline/unroll optimization, memory access patterns to verify alignment between memory partitioning parallelism, and resource saturation to determine hardware constraint compatibility (line 5). This process illustrates how LLMs explore diverse optimization directions during the search process while identifying appropriate niches for trade-offs or specialized optimizations.

Bottleneck Analysis with QoR-Aware Adaptation. When design goals remain elusive, experts adopt a systematic approach to identify critical bottlenecks and take advantage of potential optimization opportunities rather than discard existing work altogether. The *optimization trajectory reflection* provides valuable insights that guide subsequent LLM reasoning about promising design refinement. Initially, the LLM classifies designs as compute-bound or memory-bound based on QoR (line 6). For the compute-bound, the LLM progressively enhances unrolling granularity in performance-critical loops, guided by optimization trajectory analysis. For the memory-bound, the LLM adjusts memory partition factors to meet or exceed the corresponding data access unroll factors while examining nested loops to implement coarse-grained pipelining toward outer loops.

Divergence-Enhanced Design Refactoring. LLMs often show hesitance to extrapolate beyond established examples and venture into unexplored design territories. To enhance exploration coverage across the entire design space, we prompt the LLM to scrutinize current hardware optimization strategies and develop novel directive configurations different from previous iterations (line 7). Additionally, we specified the rule of first coarsely estimating the lower bound of the initiation intervals, and then applying the pipelining strategy to the innermost loop in the nested loop, while dynamically adapting memory partition factor to match loop operation characteristics. Through the shuffle of directive combinations under specific hardware optimization principles, LLM implements innovative optimization strategies for non-oriented refinement of the original design.

5 Evaluations & Discussions

In this section, we evaluate the effectiveness of iDSE in exploring Pareto-optimal designs that satisfy diverse optimization preferences. We selected 12 HLS benchmarks with varying functionality and design space dimensions $|\Phi|$ from PolyBench [90], CHStone [91], and MachSuite [92]. Diverse

Table 1: Comparison of iDSE effectiveness over baseline DSE methods.

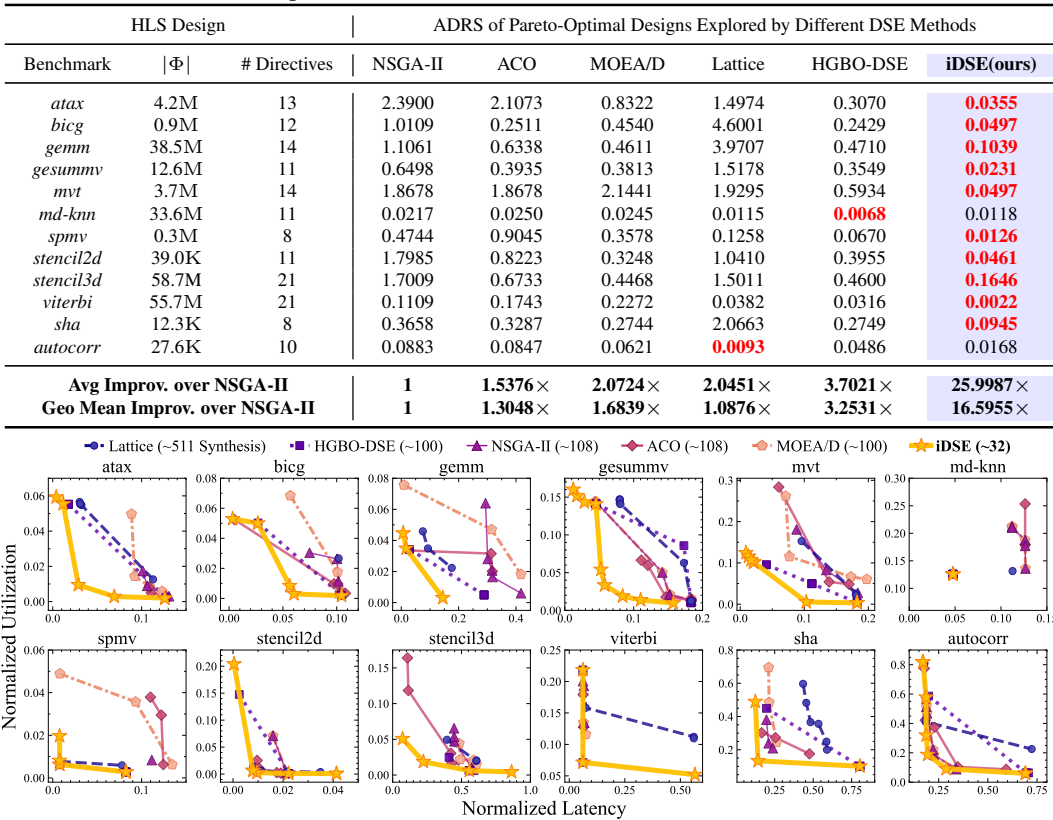


Figure 4: Comparison of explored Pareto fronts across benchmarks with different design spaces. iDSE converges to comprehensive and concave shapes with fewer search budgets (# Synthesis).

design structures and memory footprints demonstrate the robust generalization of our approach. All synthesis was performed on Vitis HLS 2022.1 [93] targeting the Xilinx ZCU106 MPSoC platform. We compared iDSE against traditional DSE methods, including evolutionary algorithms (NSGA-II [89] and MOEA/D) [68], swarm intelligence techniques (ACO) [94], and state-of-the-art approaches including Lattice [21] with guided local exploration and HGBO-DSE, a Bayesian optimization based on MOTPE [31]. iDSE consistently outperformed these methods by exploring more comprehensive and impressive Pareto fronts. Experimental results highlight the capability of iDSE as an LLM-navigated design space exploration approach that effectively unleashes the potential of LLMs in hardware optimization. The complete definitions of the benchmark design space and hyperparameter settings for heuristic-based DSE methods are detailed in Appendix C.

5.1 Navigating Design Space Exploration: Elegant and Swift Approximation of Pareto Front

We evaluated the capability of iDSE to approximate reference Pareto fronts using ADRS (complete definition is elaborated in Appendix C.1). To ensure practicality, we extensively sampled design spaces using random sampling and specialized breadth-first search to construct the reference Pareto fronts. For smaller designs (*stencil2d*, *autocorr*, and *sha*), we performed exhaustive exploration to construct strong reference Pareto fronts. All DSE methods explored design spaces compressed by our *Feature-Driven Pruning* method to ensure fair comparison. Table 1 demonstrates the superior performance of iDSE across most benchmarks. iDSE achieves geometric mean improvements of 16.6× over NSGA-II, 12.7× over ACO, 9.9× over MOEA/D, 15.3× over Lattice and 5.1× over HGBO-DSE. While Lattice achieved optimal performance in *autocorr* through local search traversal, its sensitivity to initial sampling designs and lack of global perspective limit its effectiveness in exploring trade-off curves in large memory footprints and complex design structures. Similarly, HGBO-DSE outperforms other baselines but still faces limitations when confronting vast design spaces without prior knowledge guidance. Other DSE methods compressed exploration efficiency under limited search budgets. We present full experimental details in Appendix D.

Table 3: ADRS comparison of heuristic-based DSE methods with different initial sampling.

Benchmark	NSGA-II				MOEA/D				ACO		
	RS	BS	LHS	Warm-Start	RS	BS	LHS	Warm-Start	RS	BS	LHS
<i>atax</i>	2.3900	1.1054	0.5737	0.3116	0.8322	0.4583	0.3057	0.1762	2.1073	0.9770	0.7917
<i>bicg</i>	1.0109	0.3685	1.0765	0.2428	0.4540	0.2588	0.2573	0.2758	0.2511	0.3938	0.2570
<i>gemm</i>	1.1061	0.5100	1.0581	0.4581	0.4611	0.3768	0.3664	0.2976	0.6338	0.4839	0.5489
<i>gesummv</i>	0.6498	0.6508	0.9751	0.5575	0.3813	0.4097	0.3103	0.2640	0.3935	0.4165	0.3682
<i>mvt</i>	1.8678	0.8544	0.6403	0.4193	2.1441	1.6956	0.5464	0.4976	1.8678	1.2207	0.8978
<i>md-knn</i>	0.0217	0.0208	0.0064	0.0064	0.0245	0.0184	0.0064	0.0116	0.0250	0.0218	0.0064
<i>spmv</i>	0.4744	1.0585	0.8129	0.0592	0.3578	0.8841	0.2643	0.1175	0.9045	0.9528	0.5974
<i>stencil2d</i>	1.7985	0.4616	1.2631	0.3622	0.3248	0.2991	0.3789	0.2805	0.8223	0.9477	1.3129
<i>stencil3d</i>	1.7009	0.6244	1.5550	0.1780	0.4468	0.6172	0.2057	0.2891	0.6733	0.6327	0.6682
<i>viterbi</i>	0.1109	0.1069	0.0300	0.0158	0.2272	0.1421	0.0328	0.0540	0.1743	0.1362	0.1351
<i>sha</i>	0.3658	0.1626	0.7494	0.1521	0.2744	0.0871	0.2060	0.2095	0.0847	0.2313	0.2571
<i>autocorr</i>	0.0883	0.0702	0.0931	0.7458	0.0621	0.0901	0.0901	0.0631	0.3287	0.0704	0.0642
Avg	1	1.9097\times	1.7808\times	4.6109\times	2.0724\times	2.5986\times	3.7184\times	4.2138\times	1.7401\times	1.6765\times	2.0451\times
Geo Mean	1	1.6508\times	1.3656\times	3.1709\times	1.6839\times	1.9743\times	3.1445\times	3.4065\times	1.3048\times	1.5094\times	1.8210\times

* Experiments exclude ACO with *Warm-Start* because swarm intelligence struggles to leverage the advantage of seed directive configurations, detailed results in Appendix D.3. The ADRS are calculated from the average results of 5 test runs, and *Warm-Start* are the average results of 5 rounds of DeepSeek-R1 invocations.

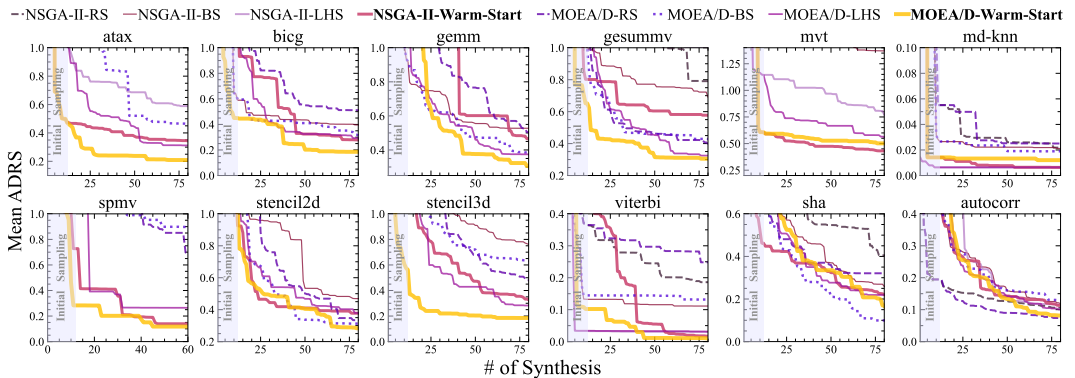


Figure 5: Comparison among EA-based DSE methods under different initial sampling designs.

Figure 4 further illustrates the advantage of iDSE in multiobjective optimization, establishing more comprehensive and concave Pareto fronts with fewer search budgets (under 50 explored designs per benchmark). Table 2 compares the number of explored designs required by different DSE methods to achieve the target ADRS. iDSE significantly enhances exploration efficiency, achieving a geometric mean speedup of 11.0 \times over meta-heuristic-based DSE methods and 4.4 \times over SOTA DSE methods. The notable improvement in performance and efficiency of iDSE stems from the dual effectiveness of initial high-quality sampling and intelligently guided searches. LLM accelerates convergence to Pareto-optimal designs that satisfy diverse optimization preferences by prudent directive combination scheduling and parameter tuning.

Table 2: Comparison of search budgets for target ADRS across different benchmarks.

DSE Methods	Poly.	Mach.	CHS.	Speedup
NSGA-II	108	108	108	1 \times
ACO	41	68	83	3.31 \times
MOEA/D	22	61	38	3.56 \times
Lattice	89	55	72	2.22 \times
HGBO-DSE	8	9	74	14.34 \times
iDSE	4	5	7	25.07\times

5.2 DSE Warm-Start: Robust Sampling Initialization for Convergence Acceleration

Heuristic-based DSE approaches often suffer from reduced convergence capabilities due to the lack of diverse and insightful initial sampling designs, which limits their ability to identify effective optimization directions. In contrast, Lattice uses U-shaped Beta sampling to strategically sample the boundaries of the design space, enabling more sensible cluster-based exploration near reference Pareto fronts. Therefore, we propose that initial sampling quality is a critical determinant of both overall DSE effectiveness and the convergence toward optimal designs. To validate our hypothesis and assess the efficacy of the *Seed Directive Generation (Warm-Start)* method, we conducted comparative analyses against Random Sampling (RS), U-shaped Beta Sampling (BS), and Latin Hypercube Sampling (LHS) within heuristic-based DSE methods. As shown in Table 3, ADRS drops substantially when seed designs more accurately approximate the reference Pareto fronts. Both BS and LHS methods

consistently outperform RS across NSGA-II, ACO, and MOEA/D. By reasoning about HLS design structure and viable optimization space, LLM optimally constructs superior approximate Pareto fronts within limited explored designs. When paired with traditional evolutionary algorithms (EA) as search engines, our method achieves sampling effects that exceed RS by $2.5\times$, BS by $1.8\times$, and LHS by $1.6\times$. For more details, please refer to Appendix D.2.

Figure 5 depicts the ADRS descent curve, showing that *Warm-Start* converges more rapidly towards reference Pareto fronts, achieving lower ADRS compared to probability distribution-based alternatives. The subsequent EA-based DSE further recovers entire Pareto fronts. More insightfully, we observed that the improved initial sampling quality produced minimal improvements for ACO. This is probably attributed to the reliance on dynamic updates during the iteration process, which gradually overrides initial path advantages through evaporation and reinforcement processes, thereby diminishing the influence of initially superior solutions (detailed evidence in Appendix D.3). In contrast, EA-based methods explicitly preserve high-quality genes, allowing the quality of seed designs to persistently guide search directions and yield more substantial improvements.

5.3 Ablation Study: Infusing Optimization Intuition into Directive Configuration Tuning

Traditional EAs, lacking domain expertise, struggle to capture the nuanced relationship of optimization directives applied to specific HLS designs. We enable more sensible directive configuration tuning by introducing LLM to infuse hardware optimization intuition. To evaluate our approach, we conducted ablation experiments with the following settings:

- *Baseline*: We prompted LLM with the HLS design and the corresponding QoR to generate directive combinations and parameters different from the initial sampling designs.
- *S1*: We incorporated information of the pruned design space to constrain exploration within reasonable boundaries, examining the effectiveness of pruning strategies on DSE.
- *S2*: We analyzed optimization trajectories of selected parents to prompt LLM to generate novel designs, examining the benefits of the *optimization trajectory reflection* on the subsequent search.
- *S3*: We further integrated bottleneck analysis and design refactoring operators, examining the enhancement effects of domain-specific hardware optimization knowledge on DSE.

The geometric mean improvement trend of ADRS in Figure 6 demonstrates that, given comparable search budgets, the proposed *QoR-Aware Adaptive Optimization (S3)* system effectively leverages prior knowledge for more efficient design space exploration. Without proper perception of design space dimensions (*Baseline*), aggressive exploration often encounters invalid designs, comprising 12.4% of total designs, degrading the efficiency of DSE. Constraining the exploration space within the ranges established by our *Feature-Driven Pruning (S1)* significantly eliminated 89.9% invalid designs. Furthermore, introducing *optimization trajectory reflection (S2)* improved the effectiveness of optimization by 20.5%. Injecting domain-specific knowledge into the search process (*S3*) further improved the effectiveness by an additional 45.0%. Additionally, our approach maintains prompt interfaces that enable further incorporation of hardware optimization preferences and resource constraints for flexible outputs.

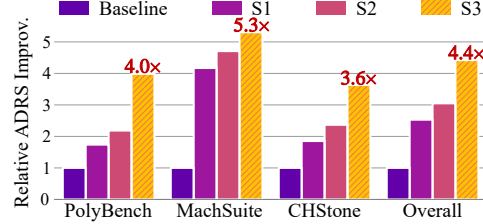


Figure 6: Ablation of Adaptive Optimization.

6 Conclusion

This paper presents iDSE, an effective and efficient LLM-navigated framework for automated high-level synthesis design space exploration, addressing the challenges of time-consuming hardware optimization with steep expertise barriers. Our approach leverages LLMs to enable elegant identification of HLS design bottlenecks and exploitation of optimization opportunities, construct representative initial sampling designs and expedite subsequent refinement within pruned design spaces. Experimental results substantiate that iDSE markedly outperforms traditional heuristic-based DSE methods, achieving superior approximation to the Pareto front with substantially reduced search budgets. Furthermore, iDSE rapidly converges to more comprehensive and compelling Pareto-optimal designs, expanding the boundary of HLS advantages in agile hardware development and optimization.

References

- [1] Norman P. Jouppi, Doe Hyun Yoon, Matthew Ashcraft, Mark Gottscho, Thomas B. Jablin, George Kurian, James Laudon, Sheng Li, Peter Ma, Ma, et al. Ten lessons from three generations shaped Google’s TPUs: Industrial product. In *2021 ACM/IEEE 48th Annual International Symposium on Computer Architecture (ISCA)*, pages 1–14, 2021.
- [2] Norman P. Jouppi, Cliff Young, Nishant Patil, David Patterson, Gaurav Agrawal, Raminder Bajwa, Sarah Bates, Suresh Bhatia, Nan Boden, Borchers, et al. In-datacenter performance analysis of a tensor processing unit. In *2017 ACM/IEEE 44th Annual International Symposium on Computer Architecture (ISCA)*, pages 1–12, 2017.
- [3] Yu-Hsin Chen, Tushar Krishna, Joel S. Emer, and Vivienne Sze. Eyeriss: An energy-efficient reconfigurable accelerator for deep convolutional neural networks. *IEEE Journal of Solid-State Circuits*, 52(1):127–138, 2017.
- [4] Ashish Gondimalla, Noah Chesnut, Mithuna Thottethodi, and T. N. Vijaykumar. SparTen: A sparse tensor accelerator for convolutional neural networks. In *Proceedings of the 52nd Annual IEEE/ACM International Symposium on Microarchitecture (MICRO)*, page 151–165, 2019.
- [5] Sixu Li, Yang Zhao, Chaojian Li, Bowei Guo, Jingqun Zhang, Wenbo Zhu, Zhifan Ye, Cheng Wan, and Yingyan Celine Lin. Fusion-3D: Integrated acceleration for instant 3D reconstruction and real-time rendering. In *2024 57th IEEE/ACM International Symposium on Microarchitecture (MICRO)*, pages 78–91, 2024.
- [6] Dongseok Im and Hoi-Jun Yoo. CamPU: A multi-camera processing unit for deep learning-based 3D spatial computing systems. In *2024 57th IEEE/ACM International Symposium on Microarchitecture (MICRO)*, pages 50–63, 2024.
- [7] Sabrina M. Neuman, Radhika Ghosal, Thomas Bourgeat, Brian Plancher, and Vijay Janapa Reddi. RoboShape: Using topology patterns to scalably and flexibly deploy accelerators across robots. In *Proceedings of the 50th Annual International Symposium on Computer Architecture (ISCA)*, 2023.
- [8] Sabrina M. Neuman, Brian Plancher, Thomas Bourgeat, Thierry Tambe, Srinivas Devadas, and Vijay Janapa Reddi. Robomorphic computing: a design methodology for domain-specific accelerators parameterized by robot morphology. In *Proceedings of the 26th ACM International Conference on Architectural Support for Programming Languages and Operating Systems (ASPLOS)*, page 674–686, 2021.
- [9] Seunghee Han, Seungjae Moon, Teokkyu Suh, JaeHoon Heo, and Joo-Young Kim. BLESS: Bandwidth and locality enhanced smem seeding acceleration for DNA sequencing. In *2024 ACM/IEEE 51st Annual International Symposium on Computer Architecture (ISCA)*, pages 582–596, 2024.
- [10] Julian Pavon, Ivan Vargas Valdivieso, Carlos Rojas, Cesar Hernandez, Mehmet Aslan, Roger Figueras, Yichao Yuan, Joël Lindegger, Mohammed Alser, Moll, et al. QUETZAL: Vector acceleration framework for modern genome sequence analysis algorithms. In *2024 ACM/IEEE 51st Annual International Symposium on Computer Architecture (ISCA)*, pages 597–612, 2024.
- [11] Max Doblas, Oscar Lostes-Cazorla, Quim Aguado-Puig, Nick Cebry, Pau Fontova-Musté, Christopher Frances Batten, Santiago Marco-Sola, and Miquel Moretó. GMX: Instruction set extensions for fast, scalable, and efficient genome sequence alignment. In *Proceedings of the 56th Annual IEEE/ACM International Symposium on Microarchitecture (MICRO)*, page 1466–1480, 2023.
- [12] Damla Senol Cali, Konstantinos Kanellopoulos, Joël Lindegger, Zülfü Bingöl, Gurpreet S. Kalsi, Ziyi Zuo, Can Firtina, Meryem Banu Cavlak, Jeremie Kim, Nika Mansouri Ghiasi, Singh, et al. SeGram: a universal hardware accelerator for genomic sequence-to-graph and sequence-to-sequence mapping. In *Proceedings of the 49th Annual International Symposium on Computer Architecture (ISCA)*, page 638–655, 2022.
- [13] Hadi Esmaeilzadeh, Emily Blem, Renee St. Amant, Karthikeyan Sankaralingam, and Doug Burger. Dark silicon and the end of multicore scaling. *IEEE Micro*, 32(3):122–134, 2012.

- [14] Yuze Chi, Weikang Qiao, Atefeh Sohrabizadeh, Jie Wang, and Jason Cong. Democratizing domain-specific computing. *Communications of the ACM*, 66(1):74–85, 2022.
- [15] Jason Cong, Bin Liu, Stephen Neuendorffer, Juanjo Noguera, Kees Vissers, and Zhiru Zhang. High-Level Synthesis for FPGAs: From prototyping to deployment. *IEEE Transactions on Computer-Aided Design of Integrated Circuits and Systems*, 30(4):473–491, 2011.
- [16] Jason Cong, Jason Lau, Gai Liu, Stephen Neuendorffer, Peichen Pan, Kees Vissers, and Zhiru Zhang. FPGA HLS today: Successes, challenges, and opportunities. *ACM Transactions on Reconfigurable Technology and Systems*, 15(4), 2022.
- [17] Benjamin Carrion Schafer, Takashi Takenaka, and Kazutoshi Wakabayashi. Adaptive simulated annealer for high level synthesis design space exploration. In *2009 International Symposium on VLSI Design, Automation and Test*, pages 106–109, 2009.
- [18] Benjamin Carrion Schafer. Parallel high-level synthesis design space exploration for behavioral IPs of exact latencies. *ACM Transactions on Design Automation of Electronic Systems (TODAES)*, 22(4), 2017.
- [19] Benjamin Carrion Schafer. Probabilistic multiknob high-level synthesis design space exploration acceleration. *IEEE Transactions on Computer-Aided Design of Integrated Circuits and Systems*, 35(3):394–406, 2016.
- [20] Qi Sun, Tinghuan Chen, Siting Liu, Jianli Chen, Hao Yu, and Bei Yu. Correlated multi-objective multi-fidelity optimization for HLS directives design. *ACM Transactions on Design Automation of Electronic Systems (TODAES)*, 27(4), 2022.
- [21] Lorenzo Ferretti, Giovanni Ansaldi, and Laura Pozzi. Lattice-traversing design space exploration for high level synthesis. In *2018 IEEE 36th International Conference on Computer Design (ICCD)*, pages 210–217, 2018.
- [22] Cody Hao Yu, Peng Wei, Max Grossman, Peng Zhang, Vivek Sarker, and Jason Cong. S2FA: An accelerator automation framework for heterogeneous computing in datacenters. In *2018 55th ACM/ESDA/IEEE Design Automation Conference (DAC)*, pages 1–6, 2018.
- [23] Yunsheng Bai, Atefeh Sohrabizadeh, Zongyue Qin, Ziniu Hu, Yizhou Sun, and Jason Cong. Towards a comprehensive benchmark for high-level synthesis targeted to FPGAs. In *Proceedings of the 37th International Conference on Neural Information Processing Systems*, 2023.
- [24] Atefeh Sohrabizadeh, Yunsheng Bai, Yizhou Sun, and Jason Cong. Automated accelerator optimization aided by graph neural networks. In *Proceedings of the 59th ACM/IEEE Design Automation Conference (DAC)*, page 55–60, 2022.
- [25] Atefeh Sohrabizadeh, Yunsheng Bai, Yizhou Sun, and Jason Cong. Robust GNN-Based representation learning for HLS. In *2023 IEEE/ACM International Conference on Computer Aided Design (ICCAD)*, pages 1–9, 2023.
- [26] Nan Wu, Yuan Xie, and Cong Hao. IronMan-Pro: Multiobjective design space exploration in HLS via reinforcement learning and graph neural network-based modeling. *IEEE Transactions on Computer-Aided Design of Integrated Circuits and Systems*, 42(3):900–913, 2023.
- [27] Jieru Zhao, Liang Feng, Sharad Sinha, Wei Zhang, Yun Liang, and Bingsheng He. COMBA: A comprehensive model-based analysis framework for high level synthesis of real applications. In *2017 IEEE/ACM International Conference on Computer-Aided Design (ICCAD)*, pages 430–437, 2017.
- [28] Guanwen Zhong, Alok Prakash, Yun Liang, Tulika Mitra, and Smail Niar. Lin-Analyzer: A high-level performance analysis tool for FPGA-based accelerators. In *2016 53nd ACM/EDAC/IEEE Design Automation Conference (DAC)*, pages 1–6, 2016.
- [29] Lorenzo Ferretti, Andrea Cini, Georgios Zacharopoulos, Cesare Alippi, and Laura Pozzi. Graph neural networks for high-level synthesis design space exploration. *ACM Transactions on Design Automation of Electronic Systems (TODAES)*, 28(2), 2022.

[30] Yunsheng Bai, Atefeh Sohrabizadeh, Zijian Ding, Rongjian Liang, Weikai Li, Ding Wang, Haoxing Ren, Yizhou Sun, and Jason Cong. Learning to compare hardware designs for high-level synthesis. In *2024 ACM/IEEE 6th Symposium on Machine Learning for CAD (MLCAD)*, pages 1–7, 2024.

[31] Huizhen Kuang, Xianfeng Cao, Jingyuan Li, and Lingli Wang. HGBO-DSE: Hierarchical gnn and bayesian optimization based hls design space exploration. In *2023 International Conference on Field Programmable Technology (ICFPT)*, pages 106–114, 2023.

[32] Xi Wang, Gwok-Waa Wan, Sam-Zaak Wong, Layton Zhang, Tianyang Liu, Qi Tian, and Jianmin Ye. ChatCPU: An agile CPU design and verification platform with LLM. In *Proceedings of the 61st ACM/IEEE Design Automation Conference (DAC)*, 2024.

[33] Ke Xu, Jialin Sun, Yuchen Hu, Xinwei Fang, Weiwei Shan, Xi Wang, and Zhe Jiang. MEIC: Re-thinking RTL debug automation using LLMs. In *Proceedings of the 43rd IEEE/ACM International Conference on Computer-Aided Design (ICCAD)*, 2025.

[34] Haoyuan Wu, Zhuolun He, Xinyun Zhang, Xufeng Yao, Su Zheng, Haisheng Zheng, and Bei Yu. ChatEDA: A large language model powered autonomous agent for EDA. *IEEE Transactions on Computer-Aided Design of Integrated Circuits and Systems*, 43(10):3184–3197, 2024.

[35] Yunda Tsai, Mingjie Liu, and Haoxing Ren. RTLFixer: Automatically fixing RTL syntax errors with large language model. In *Proceedings of the 61st ACM/IEEE Design Automation Conference (DAC)*, 2024.

[36] Yonggan Fu, Yongan Zhang, Zhongzhi Yu, Sixu Li, Zhifan Ye, Chaojian Li, Cheng Wan, and Yingyan Celine Lin. GPT4AIGChip: Towards next-generation AI accelerator design automation via large language models. In *2023 IEEE/ACM International Conference on Computer Aided Design (ICCAD)*, pages 1–9, 2023.

[37] Chengrun Yang, Xuezhi Wang, Yifeng Lu, Hanxiao Liu, Quoc V Le, Denny Zhou, and Xinyun Chen. Large language models as optimizers. *arXiv preprint arXiv:2309.03409*, 2023.

[38] Shengcai Liu, Caishun Chen, Xinghua Qu, Ke Tang, and Yew-Soon Ong. Large language models as evolutionary optimizers. In *2024 IEEE Congress on Evolutionary Computation (CEC)*, pages 1–8, 2024.

[39] Beichen Huang, Xingyu Wu, Yu Zhou, Jibin Wu, Liang Feng, Ran Cheng, and Kay Chen Tan. Exploring the true potential: Evaluating the black-box optimization capability of large language models. *arXiv preprint arXiv:2404.06290*, 2024.

[40] Tennison Liu, Nicolás Astorga, Nabeel Seedat, and Mihaela van der Schaar. Large language models to enhance bayesian optimization. *arXiv preprint arXiv:2402.03921*, 2024.

[41] Xingyu Wu, Sheng-Hao Wu, Jibin Wu, Liang Feng, and Kay Chen Tan. Evolutionary computation in the era of large language model: Survey and roadmap. *IEEE Transactions on Evolutionary Computation*, 29(2):534–554, 2025.

[42] Zijian Ding, Atefeh Sohrabizadeh, Weikai Li, Zongyue Qin, Yizhou Sun, and Jason Cong. Efficient task transfer for HLS DSE. In *Proceedings of the 43rd IEEE/ACM International Conference on Computer-Aided Design (ICCAD)*, 2025.

[43] Atefeh Sohrabizadeh, Cody Hao Yu, Min Gao, and Jason Cong. AutoDSE: Enabling software programmers to design efficient FPGA accelerators. *ACM Transactions on Design Automation of Electronic Systems (TODAES)*, 27(4), 2022.

[44] Guanwen Zhong, Vanchinathan Venkataramani, Yun Liang, Tulika Mitra, and Smail Niar. Design space exploration of multiple loops on fpgas using high level synthesis. In *2014 IEEE 32nd International Conference on Computer Design (ICCD)*, pages 456–463, 2014.

[45] Nam Khanh Pham, Amit Kumar Singh, Akash Kumar, and Mi Mi Aung Khin. Exploiting loop-array dependencies to accelerate the design space exploration with high level synthesis. In *2015 Design, Automation & Test in Europe Conference & Exhibition (DATE)*, pages 157–162, 2015.

[46] Stéphane Pouget, Louis-Noël Pouchet, and Jason Cong. A unified framework for automated code transformation and pragma insertion. In *Proceedings of the 2025 ACM/SIGDA International Symposium on Field Programmable Gate Arrays (FPGA)*, page 187–198, 2025.

[47] Stéphane Pouget, Louis-Noël Pouchet, and Jason Cong. Automatic hardware pragma insertion in high-level synthesis: A non-linear programming approach. *ACM Transactions on Design Automation of Electronic Systems (TODAES)*, 30(2), 2025.

[48] Nan Wu, Hang Yang, Yuan Xie, Pan Li, and Cong Hao. High-level synthesis performance prediction using GNNs: benchmarking, modeling, and advancing. In *Proceedings of the 59th ACM/IEEE Design Automation Conference (DAC)*, page 49–54, 2022.

[49] Ruizhe Zhong, Xingbo Du, Shixiong Kai, Zhentao Tang, Siyuan Xu, Hui-Ling Zhen, Jianye Hao, Qiang Xu, Mingxuan Yuan, and Junchi Yan. LLM4EDA: Emerging progress in large language models for electronic design automation. *arXiv preprint arXiv:2401.12224*, 2023.

[50] Zehua Pei, Hui-Ling Zhen, Mingxuan Yuan, Yu Huang, and Bei Yu. BetterV: controlled verilog generation with discriminative guidance. In *Proceedings of the 41st International Conference on Machine Learning (ICML)*, 2024.

[51] Bingkun Yao, Ning Wang, Jie Zhou, Xi Wang, Hong Gao, Zhe Jiang, and Nan Guan. Location is key: Leveraging large language model for functional bug localization in verilog. *arXiv preprint arXiv:2409.15186*, 2024.

[52] Yuchen Hu, Junhao Ye, Ke Xu, Jialin Sun, Shiyue Zhang, Xinyao Jiao, Dingrong Pan, Jie Zhou, Ning Wang, Weiwei Shan, Xinwei Fang, Xi Wang, Nan Guan, and Zhe Jiang. UVLLM: An automated universal RTL verification framework using LLMs. *arXiv preprint arXiv:2411.16238*, 2024.

[53] Sam-Zaak Wong, Gwok-Waa Wan, Dongping Liu, and Xi Wang. VGV: Verilog generation using visual capabilities of multi-modal large language models. In *2024 IEEE LLM Aided Design Workshop (LAD)*, pages 1–5, 2024.

[54] Shailja Thakur, Baleegh Ahmad, Hammond Pearce, Benjamin Tan, Brendan Dolan-Gavitt, Ramesh Karri, and Siddharth Garg. VeriGen: A large language model for verilog code generation. *ACM Transactions on Design Automation of Electronic Systems (TODAES)*, 29(3), 2024.

[55] Yuxuan Yin, Yu Wang, Boxun Xu, and Peng Li. ADO-LLM: Analog design bayesian optimization with in-context learning of large language models. In *Proceedings of the 43rd IEEE/ACM International Conference on Computer-Aided Design (ICCAD)*, 2025.

[56] Dimple Vijay Kochar, Hanrui Wang, Anantha Chandrakasan, and Xin Zhang. LEDRO: LLM-Enhanced design space reduction and optimization for analog circuits. *arXiv preprint arXiv:2411.12930*, 2024.

[57] Ning Wang, Bingkun Yao, Jie Zhou, Yuchen Hu, Xi Wang, Nan Guan, and Zhe Jiang. VeriDebug: A unified LLM for verilog debugging via contrastive embedding and guided correction. *arXiv preprint arXiv:2504.19099*, 2025.

[58] Ning Wang, Bingkun Yao, Jie Zhou, Yuchen Hu, Xi Wang, Nan Guan, and Zhe Jiang. Insights from verification: Training a verilog generation LLM with reinforcement learning with testbench feedback. *arXiv preprint arXiv:2504.15804*, 2025.

[59] Kangwei Xu, Grace Li Zhang, Xunzhao Yin, Cheng Zhuo, Ulf Schlichtmann, and Bing Li. Automated C/C++ program repair for high-level synthesis via large language models. In *Proceedings of the 2024 ACM/IEEE International Symposium on Machine Learning for CAD (MLCAD)*, 2024.

[60] Chenwei Xiong, Cheng Liu, Huawei Li, and Xiaowei Li. HLSPilot: LLM-based high-level synthesis. In *Proceedings of the 43rd IEEE/ACM International Conference on Computer-Aided Design (ICCAD)*, 2025.

[61] Haocheng Xu, Haotian Hu, and Sitao Huang. Optimizing high-level synthesis designs with retrieval-augmented large language models. In *2024 IEEE LLM Aided Design Workshop (LAD)*, pages 1–5, 2024.

[62] Neha Prakriya, Zijian Ding, Yizhou Sun, and Jason Cong. LIFT: Llm-based pragma insertion for HLS via GNN supervised fine-tuning. *arXiv preprint arXiv:2504.21187*, 2025.

[63] Hanyu Wang, Xinrui Wu, Zijian Ding, Su Zheng, Chengyue Wang, Tony Nowatzki, Yizhou Sun, and Jason Cong. LLM-DSE: Searching accelerator parameters with LLM agents, 2025.

[64] Luca Collini, Siddharth Garg, and Ramesh Karri. C2HLSC: Leveraging large language models to bridge the software-to-hardware design gap. *arXiv preprint arXiv:2412.00214*, 2024.

[65] Luca Collini, Andrew Hennessee, Ramesh Karri, and Siddharth Garg. Can reasoning models reason about hardware? an agentic HLS perspective. *arXiv preprint arXiv:2503.12721*, 2025.

[66] Xi Lin, Hui-Ling Zhen, Zhenhua Li, Qing-Fu Zhang, and Sam Kwong. Pareto multi-task learning. In *Advances in Neural Information Processing Systems*, volume 32, 2019.

[67] Xingchao Liu, Xin Tong, and Qiang Liu. Profiling pareto front with multi-objective stein variational gradient descent. In *Advances in Neural Information Processing Systems*, volume 34, pages 14721–14733, 2021.

[68] Qingfu Zhang and Hui Li. MOEA/D: A multiobjective evolutionary algorithm based on decomposition. *IEEE Transactions on Evolutionary Computation*, 11(6):712–731, 2007.

[69] Aviv Navon, Aviv Shamsian, Ethan Fetaya, and Gal Chechik. Learning the pareto front with hypernetworks. In *International Conference on Learning Representations (ICLR)*, 2021.

[70] Xi Lin, Zhiyuan Yang, Xiaoyuan Zhang, and Qingfu Zhang. Pareto set learning for expensive multi-objective optimization. In *Proceedings of the 36th International Conference on Neural Information Processing Systems*, 2022.

[71] Xiaoyuan Zhang, Xi Lin, Bo Xue, Yifan Chen, and Qingfu Zhang. Hypervolume maximization: a geometric view of pareto set learning. In *Proceedings of the 37th International Conference on Neural Information Processing Systems*, 2023.

[72] Yifan Zhong, Chengdong Ma, Xiaoyuan Zhang, Ziran Yang, Haojun Chen, Qingfu Zhang, Siyuan Qi, and Yaodong Yang. Panacea: Pareto alignment via preference adaptation for LLMs. In *Advances in Neural Information Processing Systems*, volume 37, pages 75522–75558, 2024.

[73] Seung Hyun Lee, Yinxiao Li, Junjie Ke, Innfarm Yoo, Han Zhang, Jiahui Yu, Qifei Wang, Fei Deng, Glenn Entis, Junfeng He, Gang Li, Sangpil Kim, Irfan Essa, and Feng Yang. Parrot: Pareto-optimal multi-reward reinforcement learning framework for text-to-image generation. In *European Conference on Computer Vision (ECCV)*, page 462–478, 2024.

[74] Fei Liu, Xialiang Tong, Mingxuan Yuan, Xi Lin, Fu Luo, Zhenkun Wang, Zhichao Lu, and Qingfu Zhang. Evolution of heuristics: towards efficient automatic algorithm design using large language model. In *Proceedings of the 41st International Conference on Machine Learning (ICML)*, 2024.

[75] Bernardino Romera-Paredes, Mohammadamin Barekatain, Alexander Novikov, Matej Balog, M Pawan Kumar, Emilien Dupont, Francisco JR Ruiz, Jordan S Ellenberg, Pengming Wang, Omar Fawzi, et al. Mathematical discoveries from program search with large language models. *Nature*, 625(7995):468–475, 2024.

[76] Zhi Zheng, Zhuoliang Xie, Zhenkun Wang, and Bryan Hooi. Monte carlo tree search for comprehensive exploration in llm-based automatic heuristic design. *arXiv preprint arXiv:2501.08603*, 2025.

[77] Shunyu Yao, Fei Liu, Xi Lin, Zhichao Lu, Zhenkun Wang, and Qingfu Zhang. Multi-objective evolution of heuristic using large language model. In *Proceedings of the AAAI Conference on Artificial Intelligence*, volume 39, pages 27144–27152, 2025.

[78] Haoran Ye, Jiarui Wang, Zhiguang Cao, Federico Berto, Chuanbo Hua, Haeyeon Kim, Jinkyoo Park, and Guojie Song. Reeve: Large language models as hyper-heuristics with reflective evolution. *arXiv preprint arXiv:2402.01145*, 2024.

[79] Angelica Chen, David Dohan, and David So. EvoPrompting: Language models for code-level neural architecture search. In *Advances in Neural Information Processing Systems*, volume 36, pages 7787–7817, 2023.

[80] Caiyang Yu, Xianggen Liu, Yifan Wang, Yun Liu, Wentao Feng, Xiong Deng, Chenwei Tang, and Jiancheng Lv. GPT-NAS: Neural architecture search meets generative pre-trained transformer model. *Big Data Mining and Analytics*, 8(1):45–64, 2025.

[81] Muhammad Umair Nasir, Sam Earle, Julian Togelius, Steven James, and Christopher Cleghorn. LLMatic: neural architecture search via large language models and quality diversity optimization. In *proceedings of the Genetic and Evolutionary Computation Conference*, pages 1110–1118, 2024.

[82] Haishuai Wang, Yang Gao, Xin Zheng, Peng Zhang, Hongyang Chen, Jiajun Bu, and Philip S Yu. Graph neural architecture search with gpt-4. *arXiv preprint arXiv:2310.01436*, 2023.

[83] Clint Morris, Michael Jurado, and Jason Zutty. LLM guided evolution-the automation of models advancing models. In *Proceedings of the Genetic and Evolutionary Computation Conference*, pages 377–384, 2024.

[84] Xun Zhou, Xingyu Wu, Liang Feng, Zhichao Lu, and Kay Chen Tan. Design principle transfer in neural architecture search via large language models. In *Proceedings of the AAAI Conference on Artificial Intelligence*, volume 39, pages 23000–23008, 2025.

[85] Lei Xu, Shanshan Wang, Emmanuel Casseau, and Chenglong Xiao. Intelligent4DSE: Optimizing high-level synthesis design space exploration with graph neural networks and large language models. *arXiv preprint arXiv:2504.19649*, 2025.

[86] Benjamin Carrion Schafer and Zi Wang. High-level synthesis design space exploration: Past, present, and future. *IEEE Transactions on Computer-Aided Design of Integrated Circuits and Systems*, 39(10):2628–2639, 2020.

[87] Lorenzo Ferretti, Jihye Kwon, Giovanni Ansaloni, Giuseppe Di Guglielmo, Luca P. Carloni, and Laura Pozzi. Leveraging prior knowledge for effective design-space exploration in high-level synthesis. *IEEE Transactions on Computer-Aided Design of Integrated Circuits and Systems*, 39(11):3736–3747, 2020.

[88] Aggelos Ferikoglou, Andreas Kakolyris, Dimosthenis Masouros, Dimitrios Soudris, and Sotirios Xydis. CollectiveHLS: A collaborative approach to high-level synthesis design optimization. *ACM Transactions on Reconfigurable Technology and Systems*, 18(1), 2024.

[89] K. Deb, A. Pratap, S. Agarwal, and T. Meyarivan. A fast and elitist multiobjective genetic algorithm: NSGA-II. *IEEE Transactions on Evolutionary Computation*, 6(2):182–197, 2002.

[90] Louis-Noel Pouchet and Tomofumi Yuki. PolyBench/C 4.2, 2016. Available at: <http://polybench.sf.net>.

[91] Yuko Hara, Hiroyuki Tomiyama, Shinya Honda, Hiroaki Takada, and Katsuya Ishii. CHStone: A benchmark program suite for practical C-based high-level synthesis. In *2008 IEEE International Symposium on Circuits and Systems (ISCAS)*, pages 1192–1195, 2008.

[92] Brandon Reagen, Robert Adolf, Yakun Sophia Shao, Gu-Yeon Wei, and David Brooks. Machsuite: Benchmarks for accelerator design and customized architectures. In *2014 IEEE International Symposium on Workload Characterization (IISWC)*, pages 110–119. IEEE, 2014.

[93] Vitis. Vitis High-Level Synthesis User Guide (UG1399), 2022. Available at: <https://docs.amd.com/r/2022.1-English/ug1399-vitis-hls>.

[94] Marco Dorigo, Mauro Birattari, and Thomas Stutzle. Ant colony optimization. *IEEE Computational Intelligence Magazine*, 1(4):28–39, 2006.

Appendix

Contents

A iDSE Implementation	17
A.1 Directive Function Description	17
A.2 Specific Pruning Strategies	18
A.3 Screening Mechanism for Designs with Optimization Potential	18
A.4 iDSE Hyperparameter Configurations	18
B Prompt Engineering	19
B.1 Prompt for Feature Extractor	19
B.2 Prompt for Feature-Driven Pruning	19
B.3 Prompt for Seed Directive Generation	20
B.4 Prompt for QoR-Aware Adaptive Optimization	21
C Experiment Details	23
C.1 Evaluation Metrics	23
C.2 Benchmark Descriptions and Design Structures	24
C.3 Heuristic-Based DSE Configurations	24
D Supplementary Results	24
D.1 Determination of Initial Sample Sizes	24
D.2 Construction of Pareto Front through Initial Single-Batch Sampling	25
D.3 Impact of Initial Sampling and Subsequent Search on Heuristic-Based DSE	26
D.4 Analysis of LLM Performance in DSE	28
D.5 Information of Assets	30
E Limitations and Future Work	31

A iDSE Implementation

A.1 Directive Function Description

iDSE supports three optimization directive types in Vitis HLS [93], PIPELINE and UNROLL for loops, and ARRAY_PARTITION for arrays. This can be generalized to other vendor HLS tools that support customizing microarchitectures through optimization directive tuning. Table 4 summarizes these optimization directive configurations and feature vectors generated for the case in Figure 2. Activating PIPELINE can boost throughput by overlapping time domains, while the UNROLL factor determines hardware loop parallelism. Meanwhile, ARRAY_PARTITION splits arrays to provide sufficient data bandwidth for unrolled loops. We encode PIPELINE and ARRAY_PARTITION types as discrete integer vectors, then combine these with unroll and partition factor vectors. Constructing feature vectors in the form of tuples by selecting specific numerical values from these directive configurations helps reduce unnecessary HLS domain-specific semantics in LLM reasoning.

Table 4: Optimization Directive Configuration and Generated Feature Vectors Example

Structure	Optimization Directive	Config.	Examples of Feature Vector
Loop	PIPELINE UNROLL	"off", "on" integer	{‘name’: ‘mul’, ‘pipeline’: 1, ‘unroll’: 2}
Array	ARRAY_PARTITION	"complete", "block", "cyclic" integer	{‘name’: ‘C’, ‘type’: 2, ‘dim’: 1, ‘factor’: 2}

```

1 # Project Setup
2 open_project vector_mul
3 add_files vector_mul.cpp
4 set_top vector_mul
5
6 # Solution Configuration
7 open_solution solution
8 set_part {xczu7ev-ffvc1156-2-e}
9 create_clock -period 10 -name default
10
11 # Array Partition Directives
12 set_directive_array_partition -type cyclic -factor 2 \
13 -dim 1 "vector_mul" A
14 set_directive_array_partition -type cyclic -factor 2 \
15 -dim 1 "vector_mul" B
16 set_directive_array_partition -type cyclic -factor 2 \
17 -dim 1 "vector_mul" C
18
19 # Loop Pipeline Directives
20 set_directive_pipeline "vector_mul/mul"
21
22 # Loop Unroll Directives
23 set_directive_unroll -factor 2 "vector_mul/mul"
24
25 # HLS Synthesis
26 csynth_design
27 exit

```

Listing 1: Vitis HLS Project Configuration for Vector Hadamard Product

Listing 1 presents an automatically generated Tcl script within iDSE workflow, designed to optimize the vector Hadamard product HLS design shown in Figure 2. Lines 12-17, 20, 23 correspond to the optimization directive insertion scripts generated from the example feature vectors in Table 4. Specifically, line 20 activates pipeline optimization for the *mul* loop, while line 23 implements a factor-2 parallel unrolling for this same loop. Lines 12-17 perform array partitioning on array *A*, *B*, *C*, utilizing a Cyclic partitioning strategy with a factor of 2 to ensure alignment with the data access throughput in the loop. Within the ARRAY_PARTITION directive, Cyclic creates smaller arrays by interleaving elements from the original array, while Block creates smaller arrays from consecutive blocks of the original array.

A.2 Specific Pruning Strategies

Feature-Driven Pruning method addresses the critical challenge of inefficient design space exploration by judiciously eliminating redundant or impractical directives, particularly when aggressive parallelism directives are configured within large design footprints. A primary consideration involves loop structure analysis, particularly for nested loops where indivisible loop boundaries relative to optimization constraints can lead to significant performance degradation. To mitigate this, the parameter configuration is constructed based on common factor vectors derived from array and loop bounds, ensuring alignment between optimization directives and hardware-imposed constraints.

For nested loop structures, the pruner employs intelligent rule-based elimination to prevent hardware over-utilization. When the outer loop is pipelined, inner loops are automatically fully unrolled, rendering inner loop unroll factor exploration redundant. The pruner detects such scenarios and disables unnecessary unroll directives for inner loops. Additionally, loops with large trip counts trigger pruning of aggressive parallelism configurations, guided by the intuition that excessive unrolling or pipelining often results in impractical resource consumption. This strategy balances exploration efficiency with design flexibility while allowing designers to tailor pruning decisions through a prompt interface for specialized optimization preferences.

Structural constraints further refine the pruning rules. For outer loops that are not perfect (only inner-most loop has content, no inter-loop logic and constant bounds), inner loop unrolling is prohibited. In multilayer nested loops, unrolling directives are automatically disabled for the outermost loop to prevent excessive hardware resource utilization. Outer loops containing multiple sub-loops within their bodies are restricted from unrolling. Furthermore, missing directives in configuration files are explicitly set to default values (e.g., unroll factor 0) to prevent undefined tool behaviors. For array partitioning, Complete type partitioning automatically disables partition factors.

A.3 Screening Mechanism for Designs with Optimization Potential

During non-dominated sorting, we calculate domination counts for each design and establish a domination relationship matrix. Subsequently, we categorize the front layers, placing non-dominated solutions into the first front, directly dominated solutions into the second front, and continuing this classification hierarchically. To preserve population diversity, the crowding distance calculation module evaluates solutions within identical Pareto front layers across both latency and resource consumption dimensions. After arranging the solution set along each objective dimension, crowding distances are determined by calculating Manhattan distances between adjacent solutions in the normalized objective space, with boundary designs receiving maximum priority values. Ultimately, a composite sorting strategy prioritizes solutions in lower front levels while preserving designs with greater crowding distances within the same level. This mechanism ensures both convergence and uniform distribution of solutions along the Pareto front.

A.4 iDSE Hyperparameter Configurations

iDSE employs an evolutionary algorithm driven by LLMs that employs hyperparameters shown in Table 5. We specifically set the initial number of samples to 12, and the reasons for this choice are detailed in the Appendix D.1. A fixed budget of 3 generations (I_{max}) balances design exploration effects and computational budgets. Meanwhile, the adoption of dynamic population size (P_i) allows for gradual scaling from initial exploration (N_0) to refinement. A non-dominated sorting with crowding distance metrics prioritizes Pareto-optimal solutions, while controlled injection of rank-2 suboptimal candidates C_{sub}^2 per generation maintains solution diversity.

Table 5: Hyperparameter setting in iDSE.

Hyperparameter	Description	Value
I_{max}	Number of evolutionary iterations	3
N_0	Initial sampling designs for DSE warm-start	12
P_i	Population size per iteration stage: [Init, Iteration, ...]	[12,~12]
C_{sub}^2	Suboptimal candidates selected from Rank 2 in Pareto front	3

B Prompt Engineering

This section presents our comprehensive approach to prompt LLMs in **iDSE** workflow. The following subsections detail our prompt architecture across six key LLM agents of the iDSE workflow. Each component represents a key stage in our automated DSE framework, transforming the traditional DSE methods to a more flexible LLM-navigated approach that ensures workflow robustness while remaining automated. We emphasize that the prompts we designed are not tailored to any specific benchmark. A unified prompt template is applied across all benchmarks to ensure the generalization of our methodology across diverse HLS designs. This approach objectively demonstrates the inherent capacity of LLMs in hardware optimization and design space exploration.

B.1 Prompt for Feature Extractor

In Figure 7, we present a few-shot example along with task descriptions and a structured output format used to prompt the LLM to extract key HLS design structure features. This step replaces the traditional preprocessing of the DSE method, which typically relies on the LLVM compiler to derive necessary structure information, thereby simplifying system deployment. Subsequently, a script identifies all common divisors of the target arrays and loop boundaries, thereby enabling the construction of the configurations for the optimization directives.

You function as an advanced code parser, specializing in the decomposition of arrays and loops structure in the C/C++ code.

- **Arrays:**
 - Extract the **array name**.
 - Identify the **array dimensions**.
 - Determine the **size** of each dimension.
- **Loops:**
 - Extract the **loop name**.
 - Extract **outer loop name** for the nested loop.
 - Calculate the **maximum number of iterations** for the loop.
- **Critical Constraints:**
Do not consider pointers, one-dimension array output 'dim': [1], two-dimension array output 'dim': [1, 2], etc. Keep "type": [0, 1, 2] and "pipeline": [0, 1] unchanged. Ensure you only provide the parsed data in the specified **JSON format**, with **no additional explanations**.
- **Reference:** Example Input: {sample_hls_design}; Example Output: {sample_directive_config}
- **Input:** Pending HLS design: {hls_design}
- **Expected output:**
The structured output for the parsed input code is as follows:

```
{
  "arrays": { "[array_name]": {
    "type": [0, 1, 2],
    "dim": [array_dimension],
    "factor_n": { "1": n_dimension_size,
                  "2": n_dimension_size } },
  "loops": { "[loop_name]": {
    "pipeline": [0, 1],
    "unroll": loop_trip_count,
    "outer_loop": outer_loop_name (only for nested loop) } } }
```

Figure 7: Prompt for Feature Extractor.

B.2 Prompt for Feature-Driven Pruning

In Figure 8, we prompt the LLM to leverage auxiliary pruning information in the structured JSON output from the previous step, thereby removing invalid (excessive parallelism leads to synthesis failure or duplication of optimization effects) configurations for certain optimization directives. Furthermore, we employ additional scripts to detect and eliminate potentially invalid designs within the pruned design space, as the LLM alone may not fully capture the complex interdependencies among directives. This hybrid pruning strategy preserves full automation while ensuring operational robustness throughout the optimization workflow.

You are an expert in high-level synthesis (HLS) design space exploration. Your task is to prune the provided optimization directive configuration file to reduce the design space. You will focus on optimizing three types of pragmas: array_partition, pipeline, and unroll.

- **Note:**

- For **nested loop**, set innermost loop pipeline to 1, if inner loop trip count > 32, set outer loop pipeline to 0.
- Apply loop unroll **pruning rules**:
 - If loop has variable bound or non-exclusive inner loop body (imperfect loop), set inner loop unroll to 0.
 - For 3+ level nested loops, set outermost loop unroll to 0.
 - For more than one sub loop, set outer loop unroll to 0.

The configuration file provides parameters for these pragmas:

- **array_partition:**

- **type:** Specifies the partitioning method. 0 represents complete partitioning, 1 indicates block partitioning, and 2 indicates cyclic partitioning.
- **dim:** Specifies the dimension to partition. n specifies the n-th dimension.
- **factor_n:** Indicates the partitioning factor (applied to block or cyclic partition types), 0 denotes perform no partition.
- **pipeline:** Specifies whether to pipeline the current loop.
- **unroll:** Specifies the unrolling factor for the current loop.

- **Input:** HLS Design Code: {hls_design};

Initial Optimization Directive Configuration File (JSON): {original_pragma_config}

- **Expect Output:**

The updated configuration file in **JSON format**.

```
{
  "arrays": { "[array_name]": {
    "type": [partition_type],
    "dim": [array_dimension],
    "factor_n": { "1": [pruned_partition_factor], ... } },
  "loops": { "[loop_name]": {
    "pipeline": [pipeline_value],
    "unroll": [pruned_unroll_factor],
    "outer_loop": outer_loop_name (only for nested loop) } } }
```

Figure 8: Prompt for Feature-Driven Pruning.

B.3 Prompt for Seed Directive Generation

Figure 9 details our hierarchical prompt architecture integrating task descriptions, sampling objectives, and functional descriptions of optimization directives. The sampling objectives are organized through three meticulously defined optimization regimes:

- **Prioritize Performance.** Maximize computational throughput through aggressive parallelism, accepting elevated resource utilization.
- **Prioritize Resource Utilization.** Minimize hardware consumption via conservative parallelism allocation, prioritizing area efficiency over high performance.
- **Performance-Cost Trade-off.** Identify unroll factor configurations that strike a feasible balance between performance and hardware resource budgets.

These distinct objectives help ensure that the initial sampling designs achieve broad coverage of the Pareto front. Furthermore, the embedded directive specifications ground LLM reasoning in domain-specific HLS constraints, and bridge the semantic gap between natural language instructions and hardware synthesis requirements through structured knowledge injection.

You are tasked with generating {num_sample} unique and effective pragma configuration combinations for optimizing the provided High-Level Synthesis (HLS) design. These configurations must target the following optimization goals while strictly adhering to the condition that only parameters available in the provided configuration file can be used.

- **Note:**

- **Performance Optimization:** Achieve the best performance, which will result in higher hardware consumption.

- **Resource Utilization Optimization:** Minimize hardware resource usage, which may result in reduced

performance.

- **PPA Tradeoff Optimization:** Find a balanced unroll factor combination that offers a good tradeoff between performance and hardware utilization.

The configuration file provides parameters for pragmas:

< Directive configuration ... >

Make Sure every loop and array (every dim) has its configuration. IF you think it's unnecessary, set corresponding unroll and factor to 0.

- **Input:** HLS Design Code: {hls_design}; Pragma parameter you can pick: {pragma_config}

- **Expect Output:**

```
[{{{'name': [loop_name], 'pipeline': [value], 'unroll': [value]}}, {...}},  
 {'name': [array_name], 'type': [value], 'dim': [value], 'factor': [value]}}, {...}}, ... ]
```

Figure 9: Prompt for Seed Directive Generation.

B.4 Prompt for QoR-Aware Adaptive Optimization

In this section, we present in detail the prompts in our *QoR-Aware Adaptive Optimization* system. In Figure 10, the hierarchical structure of prompt for **optimization trajectory reflection** comprises:

- **Parent Selection Mechanism.** A rule-based prioritization balancing Pareto dominance and solution diversity for parental candidate selection.
- **Bottleneck Identification.** Systematic bottleneck identification targeting loop optimization, memory access patterns, and resource saturation thresholds to guide iterative refinements.
- **QoR-Aware Adaptation:** Synthesized circuit performance metrics (e.g., latency and resource utilization) link directive configurations to hardware implementation evaluations, allowing LLMs to trace optimization causality quantitatively.

We are conducting HLS design space exploration. Select at least {parent_num} optimal parental candidates from the provided configuration for subsequent crossover and mutation operations. Prioritize solutions demonstrating strong Pareto dominance characteristics and preservation of solution diversity. Evaluate and analyze the bottlenecks that still exist at your selected candidate points to provide a sufficiently informative reference for the subsequent optimization, with around 3 sentences of analysis for each selected point.

- **Selection Principle:**

- **Primary Sorting Criteria:**

- Non-dominated Rank Priority (Lower rank = Higher priority)
- Crowding Distance Comparison (Higher distance = Better diversity)

- **Multi-Objective Analysis:**

- For equal-rank: Prefer configurations with higher crowding distances to maintain population diversity
- Across different ranks: Favor lower-rank solutions even with lower crowding distances

- **Bottleneck Analysis Reasoning:**

- **Step 1:** Loop Optimization Check. Check loop-carried dependencies blocking pipeline/unroll optimizations.

- **Step 2:** Memory Access Check. Verify array partitioning factors match unroll/pipeline parallelism.

- **Step 3:** Resource Saturation Check Resource Saturation. Identify DSP/BRAM overuse from aggressive unrolling or mismatched partitioning.

- **Configuration Parameters Description:** < Directive configuration ... >

- **Input:** Input Sample Configuration and Corresponding QoR: {sample_config};
HLS Design Structure: {kernel_code}

- **Expect Output:** Format selected parents with selection rationale:

```
[{ "combination_index": [int],  
  "loop_combination": [Full original structure],  
  "array_combination": [Original structure],  
  "selection_reason": {  
    "dominance_characteristic": "Pareto Rank | Crowding Distance Comparison",  
    "optimization_potential": "[identify current computation/memory_access bottleneck]"...}...]
```

Figure 10: Prompt for optimization trajectory reflection.

In Figure 11, we prompt the LLM for **bottleneck analysis with QoR-aware adaptation**. It first identify compute/memory bottlenecks in selected HLS designs with optimization potential, and then perform oriented optimizations. To maintain genetic stability, we enforce a parameter preservation by retaining a sufficient subset of parent configurations.

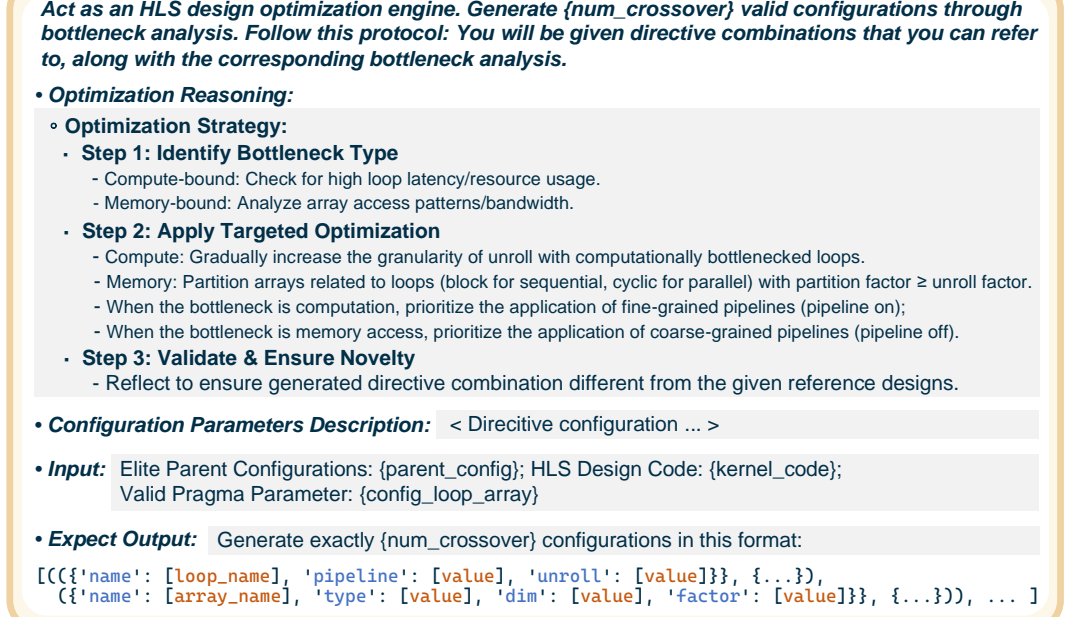


Figure 11: Prompt for bottleneck analysis with QoR-aware adaptation.

In Figure 12, we prompt the LLM for **divergence-enhanced design refactoring** to move beyond the constrained design space and generate novel directive configurations. This approach generates configurations distinct from selected parent patterns. We prioritize loop optimizations while enforcing hardware scheduling constraints to ensure design feasibility. For example, restrictions are imposed on outer loop operations through trip count threshold control, enforcing the power-of-two property of the unfolding factor, and differentiating partition type selection based on the array dimension property.

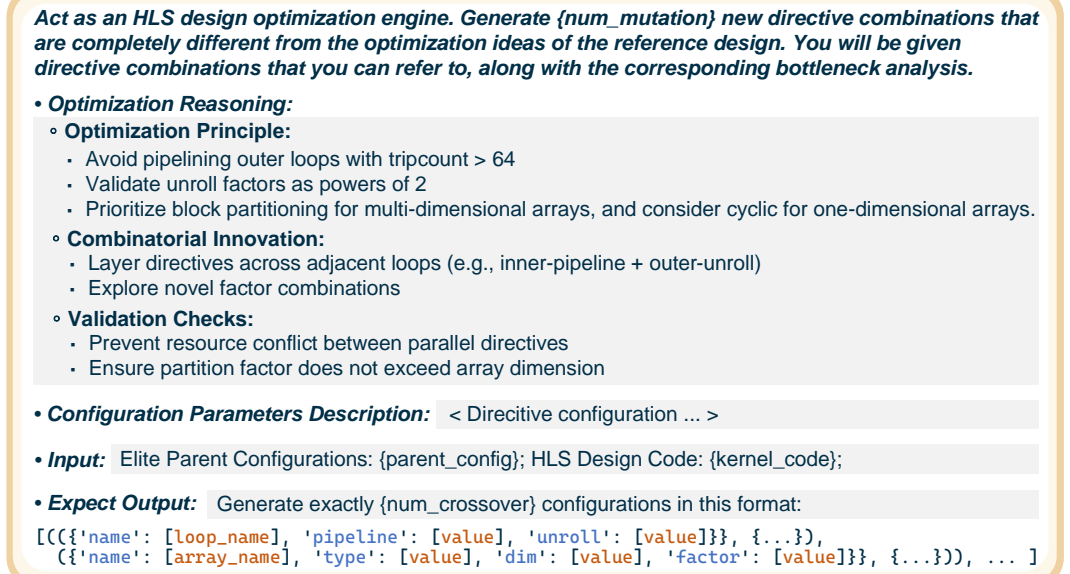


Figure 12: Prompt for divergence-enhanced design refactoring.

C Experiment Details

All experiments were conducted on an Intel Xeon Platinum 8378A server running Ubuntu 20.04.6. The designs were implemented using Vitis HLS 2022.1, targeting the Xilinx ZCU106 MPSoC platform under a maximum synthesis time constraint of 20 minutes. Evaluation of explored directive configurations exceeding this threshold typically resulted from excessively aggressive parallelization strategies that surpassed the available hardware resources.

C.1 Evaluation Metrics

The average distance to reference set (ADRS) is a widely adopted metric in High-Level Synthesis (HLS) to evaluate the quality of design space exploration (DSE). This metric quantifies the gap between an explored Pareto front P_E , generated by a DSE method, and a reference Pareto front P_R , which represents the best-known optimal solutions. ADRS is defined as the average normalized distance from each design in P_R to its closest counterpart in P_E . Formally, the metric is computed by averaging the minimum relative degradation across all objectives for every reference design, ensuring a reasonable comparison that accounts for the latency (Lat) and resource utilization ($Util$) trade-offs.

$$ADRS(P_E, P_R) = \frac{1}{|P_R|} \sum_{\lambda(\varphi^\gamma) \in P_R} \min_{\lambda(\varphi^\omega) \in P_E} d \quad (4)$$

The distance $d(\cdot)$ in ADRS is designed to measure the relative degradation of solutions in P_E compared to those in P_R . For a reference design $\lambda(\varphi^\gamma) \in P_R$, the distance to its nearest neighbor $\lambda(\varphi^\omega) \in P_E$ is calculated by taking the maximum relative difference in latency and resource utilization. This difference is normalized by the objective values of reference design to ensure scale invariance, avoiding bias toward objectives with large ranges. Critically, $d(\cdot)$ only penalizes solutions in P_E that underperform relative to P_R . If a design in P_E dominates or matches the reference design in both objectives, the distance is zero. This evaluation aligns with practical DSE goals, where the primary focus is to approximate or exceed the reference front rather than explore regions beyond it.

$$d = \max \left\{ 0, \frac{Lat(\mathcal{H}, \lambda(\varphi^\omega)) - Lat(\mathcal{H}, \lambda(\varphi^\gamma))}{Lat(\mathcal{H}, \lambda(\varphi^\gamma))}, \frac{Util(\mathcal{H}, \lambda(\varphi^\omega)) - Util(\mathcal{H}, \lambda(\varphi^\gamma))}{Util(\mathcal{H}, \lambda(\varphi^\gamma))} \right\} \quad (5)$$

ADRS is suitable for HLS DSE due to the inherent irregularities in Pareto fronts generated during exploration. In HLS, the interplay between compiler optimizations, resource constraints, and latency-performance trade-offs often leads to non-smooth, discontinuous, or clustered Pareto fronts. Traditional metrics like hypervolume (HV), which measures the volume of the objective space dominated by a Pareto front, struggle to provide reliable comparisons in such scenarios. The sensitivity of HV to the shape and continuity of the front requires convexity and smoothness for meaningful interpretation, rendering it less effective when fronts exhibit abrupt transitions or sparse distributions. In contrast, ADRS circumvents these limitations by focusing on pairwise proximity between P_E and P_R , making it robust to irregularities in the front geometry.

In the context of HLS design evaluation, the latency (Lat) is derived from synthesis timing analysis rather than post-implementation routing delays. This metric captures intrinsic circuit performance determined by logic-level optimization decisions, eliminating variations introduced by layout and wiring during the implementation phase. For resource utilization ($Util$), we define it as a weighted sum of critical FPGA schedulable resources. The utilization metric is formulated as:

$$Util(\mathcal{H}, \lambda(\varphi)) = W_{LUT} \cdot LUT + W_{FF} \cdot FF + W_{DSP} \cdot DSP + W_{BRAM} \cdot BRAM \quad (6)$$

where LUT , FF , DSP , and $BRAM$ represent the normalized usage ratios of lookup tables, flip-flops, digital signal processors, and block RAMs, respectively. The weighting coefficients ($W_{LUT} = 0.3$, $W_{FF} = 0.25$, $W_{DSP} = 0.3$, $W_{BRAM} = 0.05$) prioritize DSP and LUT resources due to their stronger correlation with computational throughput, while BRAM allocation is discounted as memory blocks are typically optimized separately through dedicated directives. By calibrating weights to specific hardware resources, it formalizes how HLS compiler decisions inherently balance computational density and memory bandwidth availability during design exploration.

C.2 Benchmark Descriptions and Design Structures

Table 6: Benchmark description with design structure.

Benchmark	Description	# Loop	# Array
<i>atax</i>	Dual matrix-vector multiplications $y = A^T(Ax)$	4	4
<i>bicg</i>	Biconjugate gradient stabilized method $q = Ap, s = A^T r$	3	5
<i>gemm</i>	BLAS general matrix multiply $C_{out} = \alpha AB + \beta C$	4	3
<i>gesummv</i>	Summed matrix-vector multiplications $y = \alpha Ax + \beta Bx$	2	5
<i>mvt</i>	Dual matrix-vector products $x1 = x1 + Ay1, x2 = x2 + A^T y2$	4	5
<i>md-knn</i>	Molecular dynamics force computation with neighbor lists	2	7
<i>spmv</i>	Sparse matrix-vector multiplication	2	4
<i>stencil2d</i>	2D convolution with 3x3 kernel	4	3
<i>stencil3d</i>	3D stencil computation with two coefficients	9	3
<i>viterbi</i>	Dynamic programming for optimal hidden state sequence in HMM	7	6
<i>sha</i>	SHA-1 cryptographic hash computation rounds	6	3
<i>autocorr</i>	Autocorrelation computation with scaling and lag products	6	0

C.3 Heuristic-Based DSE Configurations

Table 7: Baseline DSE method hyperparameter setting.

Baseline	Hyperparameter Settings
NSGA-II	<i>Initial samples = 12, Total generations = 8, Crossover probability = 0.9, Mutation probability = 0.3</i>
MOEA/D	<i>Population size=12, Max evaluations=100, Neighbor size=5, Mutation rate=0.1, Tchebycheff decomposition</i>
ACO	<i>Iterations=8, Ants=12, Evaporation rate=0.1, Pheromone update Q=100, Initial pheromone=1.0</i>
Lattice [21]	<i>Initial Beta sampling ($\alpha=0.1, \beta=0.1$), Max samples=100, Lattice radius=0.5, SphereTree neighbor search</i>
HGBO [31]	<i>LHS init trials=10, Total trials=100, EHVI candidates=24, Prior weight=1.0</i>

D Supplementary Results

D.1 Determination of Initial Sample Sizes

Our experimental observations reveal that increased initial sampling quantities generally enhance Pareto front coverage across benchmarks, as indicated by the progressive convergence toward reference fronts through diminishing ADRS values, as shown in Figure 13. While this trend demonstrates that approximation quality improves with sample size, strictly monotonic ADRS reduction does not universally occur. Furthermore, excessive sampling leads to output truncation and quality degradation due to the inherent limitations in the long-context processing capabilities of LLM. Through evaluation of the trade-off between coverage and computational complexity, we identified an optimal configuration of 12 initial samples that effectively balances approximation fidelity with computational efficiency. To ensure fair comparison across experimental evaluations, we uniformly applied this sample quantity across various heuristic-based DSE methods. This initialization strategy facilitates effective warm-start exploration while maintaining minimal computational budgets, highlighting both the efficacy of our sampling approach and the overall efficiency of **iDSE**.

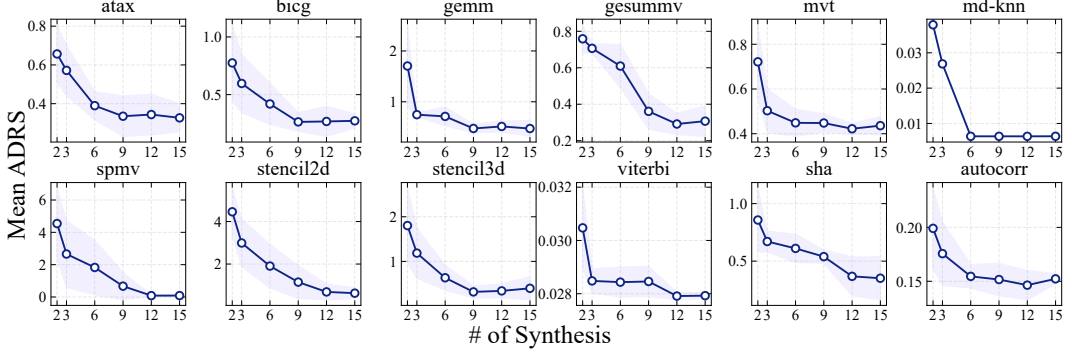


Figure 13: Optimal initial sample size selection for efficient Pareto front coverage

D.2 Construction of Pareto Front through Initial Single-Batch Sampling

In this section, we present detailed analysis of the data shown in Table 2. For our experiments, we configured NSGA-II with 12 initial sampling designs for each benchmark, eventually reaching approximately 108 populations. The ADRS explored during the DSE process serves as our comparative baseline. Table 8 enumerates the number of explored designs required by ACO, MOEA/D, Lattice, and HGBO-DSE to reach or fall below the target ADRS. When these DSE methods failed to meet the target ADRS within the limited search budget, we defined the result as the maximum population size of the baseline method. The results demonstrate that iDSE significantly outperforms other DSE methods, achieving efficiency improvements of $25.1 \times$ over NSGA-II, $7.6 \times$ over ACO, $7.0 \times$ over MOEA/D, $11.3 \times$ over Lattice, and $1.7 \times$ over HGBO-DSE. Notably, we observed that the ADRS threshold established in the baseline was consistently achieved across all benchmarks during just the *Warm-Start* phase of iDSE. This finding primarily reveals that our LLM-guided **Seed Directive Generation** method can construct superior Pareto fronts through single-batch sampling. Furthermore, it highlights the great potential of iDSE for enhancing DSE efficiency, surpassing subsequent *adaptive optimization* phases by providing designers with insightful designs in earlier stages.

Table 8: Number of explored designs required by different DSE methods to reach target ADRS.

DSE Methods	PolyBench [90]					MachSuite [92]					CHStone [91]		Speedup	
	atax	bicg	gemm	gesummv	mvt	md-knn	spmv	stencil2d	stencil3d	viterbi	sha	autocorr	Avg	Geo Mean
NSGA-II	108	108	108	108	108	108	108	108	108	108	108	108	1	1
ACO	19	2	9	67	108	108	108	9	8	108	61	105	8.80 \times	3.31 \times
MOEA/D	18	14	9	55	13	108	46	20	25	108	39	36	4.65 \times	3.56 \times
Lattice	13	108	108	108	108	93	2	59	99	23	108	36	6.59 \times	2.22 \times
HGBO-DSE	3	2	4	25	5	1	1	11	21	9	81	66	32.40 \times	14.34 \times
iDSE	3	3	6	4	5	5	1	6	3	10	6	7	30.54 \times	25.07 \times

Figure 14 illustrates the initial explored Pareto fronts obtained from different benchmarks under the previously determined number of initial samples. As shown, the *Random Sampling (RS)*, *U-shaped Beta Sampling (BS)*, and *Latin Hypercube Sampling (LHS)* methods depend solely on probabilistic distributions, producing sparsely distributed and irregularly scattered designs. Consequently, these methods struggle to achieve sufficiently broad coverage or to closely approximate the reference Pareto front. In contrast, our *Seed Directive Generation* approach leverages domain-specific prior knowledge to guide single-batch sampling, shaping a more comprehensive and more concave Pareto front that incorporates multiple promising design configurations. This comparative analysis confirms that, even during the preliminary stages of exploration, our approach achieves close alignment with the ground-truth Pareto front while incurring minimal HLS compilation overhead. The results underscore the critical role of representative seed designs in accelerating early-phase design space exploration without compromising solution quality. iDSE significantly improves exploration efficiency through initial sampling warm-start for rapid approximation of the reference Pareto fronts. This indicates that iDSE can rapidly converge, thereby reducing the time overhead required for hardware optimization while avoiding potential degradation issues that might arise from long-context prompts to LLMs.

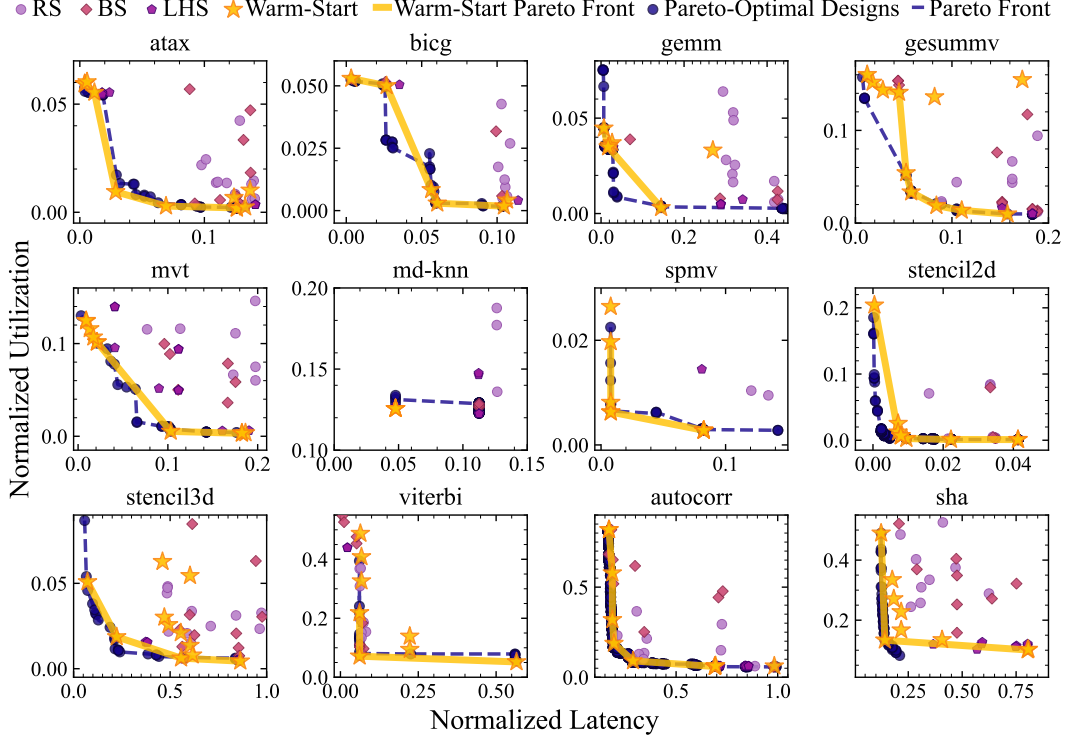


Figure 14: Comparison of Pareto fronts constructed by different initial sampling designs

D.3 Impact of Initial Sampling and Subsequent Search on Heuristic-Based DSE

To further validate our hypothesis that retaining advantageous genetic factors (partial parallelism for arrays, loops) can effectively leverage evolutionary algorithms for DSE in hardware optimization tasks, we decomposed the data in Table 3 into two distinct phases: an initial sampling phase (Table 9) and a subsequent search phase (Table 10). Our analysis reveals that the quality of sampling designs improves proportionally with the enhanced rationality of the sampling methodology. Notably, NSGA-II demonstrates a dependency between the effectiveness of its subsequent search and the quality of initial sampling, suggesting that this heuristic successfully preserves superior genetic factors during optimization to drive efficient DSE. In contrast, in ACO, the ADRS values obtained during the search phase exhibit no clear correlation with the initial sampling quality. The improvements in the quality and dispersion of the initial sampling design provided by BS and LHS compared to RS are not reflected in the subsequent search phases of ACO, as evidenced by the lack of significant differences among the indicators in the last three columns of Table 10. Unlike evolutionary algorithms that directly inherit and recombine population genes through crossover and mutation operations, ACO relies on the accumulation and evaporation of pheromone trails. While initial sampling designs may provide some prior information, the algorithm continuously weakens the influence of historical paths through pheromone evaporation mechanisms, while dynamically covering trajectories in low-quality regions through path reconstruction. This mechanism causes ACO to rely more on real-time feedback during the iteration process rather than the static distribution of the initial population. This empirical observation reinforces the rationale behind our methodology, which combines

Table 9: ADRS comparison of different initial sampling methods.

Benchmark	RS	BS	LHS	Warm-Start
atax	2.3900	1.1054	0.5737	0.3116
bicg	1.0109	0.3685	1.0765	0.2428
gemm	1.1061	0.5100	1.0581	0.4581
gesummv	0.6498	0.6508	0.9751	0.5575
mvt	1.8678	0.8544	0.6403	0.4193
md-knn	0.0217	0.0208	0.0064	0.0064
spmv	0.4744	1.0585	0.8129	0.0592
stencil2d	1.7985	0.4616	1.2631	0.3622
stencil3d	1.7009	0.6244	1.5550	0.1780
viterbi	0.1109	0.1069	0.0300	0.0158
sha	0.3658	0.1626	0.7494	0.1521
autocorr	0.0883	0.0702	0.0931	0.7458
Avg	1	1.9097 ×	1.7808 ×	4.6109 ×
Geo Mean	1	1.6508 ×	1.3656 ×	3.1709 ×

Table 10: ADRS comparison of search efficiency.

Benchmark	NSGA-II				MOEA/D				ACO		
	RS	BS	LHS	Warm-Start	RS	BS	LHS	Warm-Start	RS	BS	LHS
<i>atax</i>	2.3900	1.1054	0.5767	0.3513	0.9146	0.5794	0.5718	0.2536	2.5109	1.8452	2.5571
<i>bicg</i>	1.0109	0.4150	1.0771	0.2463	0.5229	0.3147	0.4738	0.3212	0.2711	0.4205	0.3480
<i>gemm</i>	1.1065	0.5250	1.0584	0.4581	0.5240	0.5658	0.6137	0.9358	0.6785	0.5699	0.7181
<i>gesummv</i>	0.6498	0.6595	0.9752	0.5579	0.4671	0.4182	0.3954	0.3761	0.4124	0.4188	0.4248
<i>mvt</i>	1.8678	0.8715	0.6403	0.4420	2.7230	3.5088	3.8933	3.0261	2.0321	2.0427	1.6964
<i>md-knn</i>	0.0217	0.0216	0.0064	0.0064	0.0246	0.0224	0.0306	0.0526	0.0250	0.0232	0.0215
<i>spmv</i>	0.4744	1.0585	0.8182	0.0592	0.3582	1.1170	1.3312	0.5785	1.0334	1.7828	1.3483
<i>stencil2d</i>	1.8879	0.5093	1.2729	0.3764	0.3378	0.6214	0.6710	0.4525	0.8438	1.1927	1.5266
<i>stencil3d</i>	1.7030	0.6244	1.5572	0.1780	0.4583	0.6682	0.3659	0.4397	0.7114	0.6358	0.7699
<i>viterbi</i>	0.1111	0.1206	0.2769	0.0158	0.2327	0.2502	0.2460	0.1270	0.1743	0.1363	0.1428
<i>sha</i>	0.3658	0.1626	0.7494	0.7458	0.2790	0.1302	0.2152	0.2095	0.3946	0.2313	0.2584
<i>autocorr</i>	0.0913	0.0702	0.0933	0.1521	0.0726	0.0966	0.1254	0.0673	0.0865	0.0828	0.0737
Avg	1	1.8492 ×	1.5113 ×	4.4010 ×	1.9408 ×	1.8798 ×	1.8042 ×	2.4461 ×	1.4485 ×	1.4221 ×	1.3544 ×
Geo Mean	1	1.6026 ×	1.1404 ×	3.1335 ×	1.5510 ×	1.4415 ×	1.3004 ×	1.6552 ×	1.2223 ×	1.2368 ×	1.2046 ×

LLM-enhanced initial sampling with subsequent genetic-inspired search algorithms to effectively explore high-quality designs.

Lattice achieves favorable ADRS in smaller-scale designs by utilizing U-shaped Beta sampling [21]. This sampling approach is based on prior optimization experience that designs with either very high or very low parallelism often occupy opposite ends of the Pareto front (performance-optimal with higher hardware consumption versus resource-efficient with performance trade-offs). U-shaped Beta sampling (BS) generates the initial configuration set φ^0 and derives the approximation of the Pareto front. For a sampling size N_0 , the space φ^0 comprises n unique feature vectors φ , where each element of φ is sampled probabilistically from a symmetric Beta distribution. The probability density function is defined over $0 \leq x \leq 1$ as:

$$\varphi^0(x) = \frac{x^{\alpha-1}(1-x)^{\alpha-1}}{B(\alpha)}, \quad (7)$$

$$B(\alpha) = \int_0^1 x^{\alpha-1}(1-x)^{\alpha-1} dx. \quad (8)$$

where $B(\alpha)$ denotes the Beta function. This U-shaped distribution (with $\alpha < 1$) assigns higher probability density to boundary values of x . This sampling strategy ensures that the initial feature vectors φ^0 contain extreme parameter values with high likelihood, intentionally reserving intermediate feature combinations for exploration during subsequent refinement stages.

The uniform random sampling (RS) strategy generates independent feature vectors φ^0 by selecting each parameter φ_j (for $j = 1, \dots, d$ dimensions) from a uniform distribution.

Latin Hypercube Sampling (LHS) enforces stratified spatial coverage in d -dimensional space through orthogonal permutation:

$$\varphi_{ij}^0 = \frac{\pi_j(i) - u_{ij}}{n}, \quad u_{ij} \sim \mathcal{U}(0, 1) \quad (9)$$

where $\pi_j(\cdot)$ denotes a random permutation function for the j -th dimension, and $u_{ij} \sim \mathcal{U}(0, 1)$ denotes uniformly distributed stochastic offsets within hypercube cells.

Seed Directive Generation approach (*Warm-Start*) integrates a generative model $\pi_\theta(\cdot)$, a prompt \mathcal{P} encoding task constraints, and prior knowledge of hardware optimization \mathcal{K} . Its sampling mechanism is governed by:

$$\varphi_i^0 \stackrel{\text{i.i.d.}}{\sim} \pi_\theta(\cdot \mid \mathcal{P}, \mathcal{K}) \quad (10)$$

where φ_i denotes a d -dimensional feature vector. LLMs achieve superior efficiency by integrating domain knowledge and constrained optimization principles, outperforming other sampling baselines.

D.4 Analysis of LLM Performance in DSE

In this section, we provide additional experimental results to elucidate LLM performance during the *Preprocessing*, *Warm-Start*, and *Adaptive Optimization* phases of DSE tasks. We also conduct extensive comparisons with current state-of-the-art general-purpose LLMs.

We provide supplementary data for Figure 6 in our ablation study. To validate the effectiveness of our **Feature-Driven Pruning** method, we compared the design space dimension in the *Adaptive Optimization* phase with and without pruning. We recorded the number of invalid designs that failed due to synthesis timeout or failure caused by scheduling excessive parallelism directives, as shown in Figure 15. The experimental results demonstrate that for benchmarks with larger design spaces and nested loops with high trip counts (*gemm*, *spmv*, *stencil3d*, *viterbi*), the *w/o Pruning* approach encountered numerous invalid designs. This occurs because existing LLMs struggle to capture the semantics of complex HLS DSE tasks and lack specialized hardware optimization knowledge. Consequently, they fail to establish awareness of QoR feedback during exploration, becoming lost in the vast design space. In contrast, constraining exploration to the pruned design space allows LLMs to explore directive parallelism within a restricted feasible region. This approach prevents wasted computational resources resulting from aggressive parallelism allocation or redundant directive configurations that lead to failed QoR evaluations of candidates. Moreover, our experimental results indicate that this mild pruning strategy not only significantly reduces invalid designs but also maintains excellent DSE performance, as evidenced by further improvements in Figure 6.

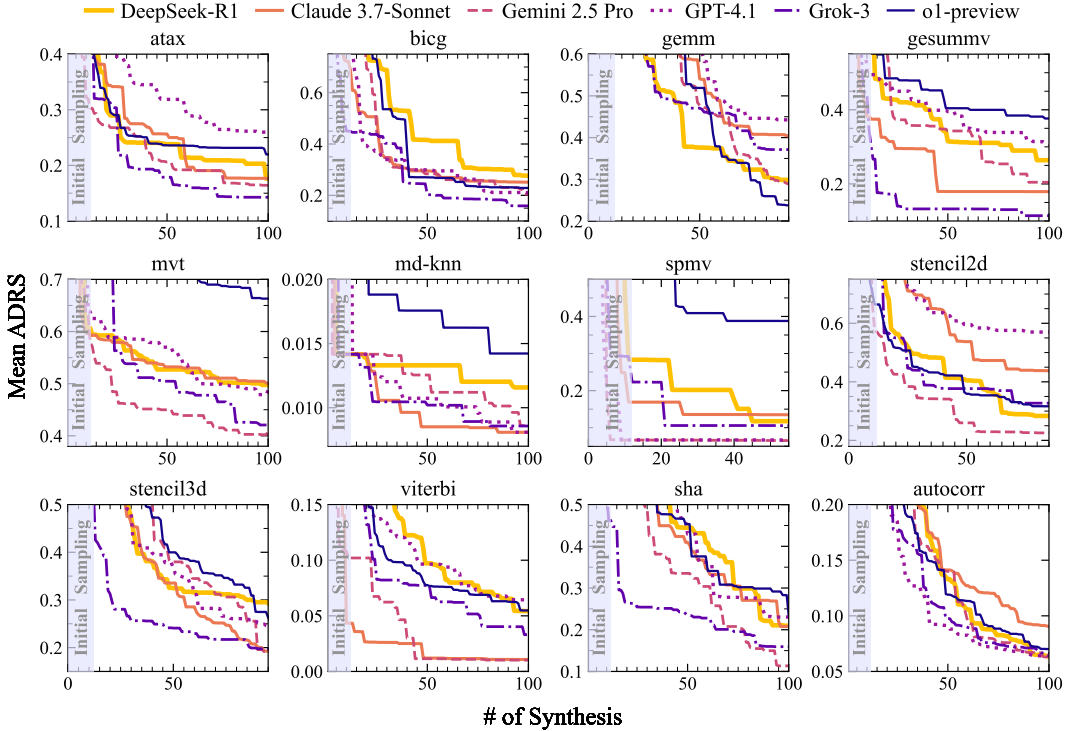


Figure 16: Comparison of ADRS among MOEA/D-based DSE method under different LLMs.

We validated our approach across multiple inference LLMs, comparing various general-purpose LLMs including *DeepSeek-R1*, *Claude 3.7-Sonnet*, *Gemini 2.5 Pro*, *GPT-4.1*, *Grok-3*, and *o1-preview* for DSE. As training scales expand and methodologies evolve, LLMs show increasing promise for driving effective DSE. Importantly, we believe that the vast HLS design space prevents LLMs from memorizing optimal directive configurations during pre-training. Instead, LLMs allocate these configurations based on learned hardware optimization principles, preserving the flexibility and generalization of iDSE.

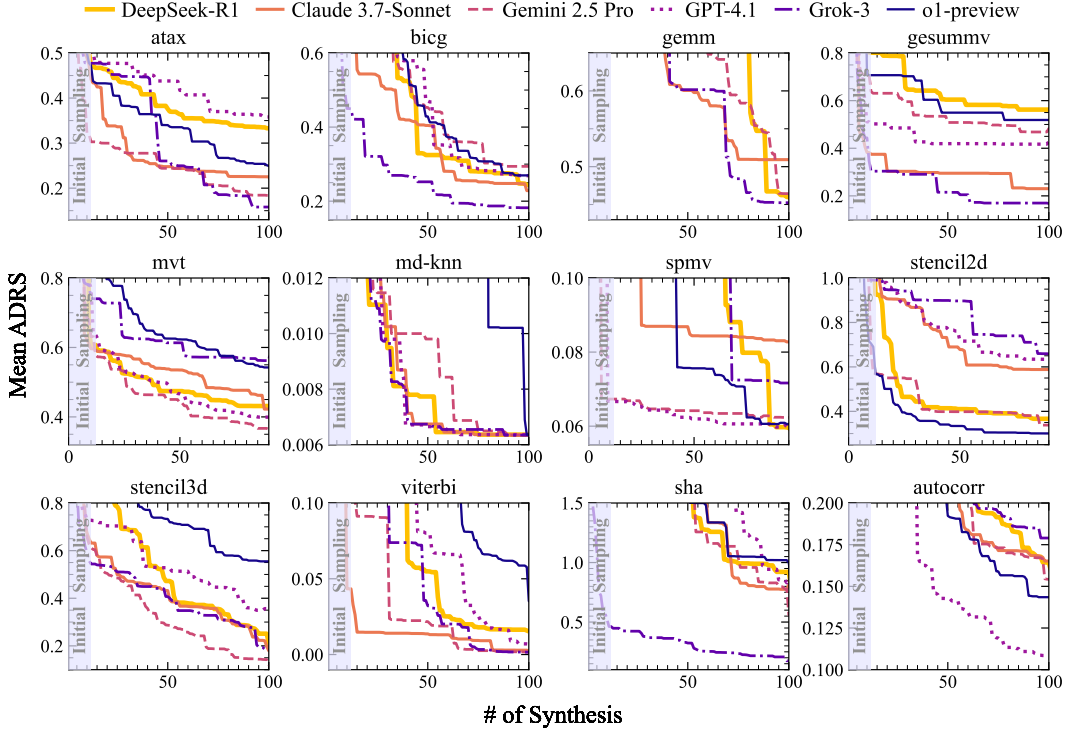


Figure 17: Comparison of ADRS among NSGA-II-based DSE method under different LLMs.

We compared different general-purpose LLMs for initial sampling, followed by EA-based DSE methods implemented with MOEA/D (Figure 16) and NSGA-II (Figure 17) for searching new directive configurations. Our experiments revealed significant variations in both convergence speed and final optimization quality across different LLMs. Notably, we found that no single model consistently outperformed others across all benchmarks, indicating that LLMs exhibit different optimization reasoning patterns depending on the HLS design structure and design space dimension.

Figure 18 compares the t-SNE visualization of feature vectors from Pareto-optimal directive configurations sampled through exhaustive exploration (approximately 10,000 explored designs per benchmark) against those identified by our method during both initial sampling and search phases. t-SNE is a dimensionality reduction technique that represents high-dimensional data as points in a two-dimensional space, where proximity between points indicates similarity in the data, while greater distances suggest dissimilarity. The visualization reveals that the design space formed by HLS optimization directives along with their parameters and combinations is exponentially large, making feature differentiation challenging and resulting in irregular visualization patterns. Furthermore, most HLS designs exhibit clustering characteristics among Pareto-optimal directive configurations. Our *Warm-Start* strategy effectively occupies these optimal design regions, thereby guiding subsequent *Adaptive Optimization* phases toward broader coverage. Comparative analysis with Figure 4 demonstrates that while our method may not comprehensively cover the extensive Pareto-optimal designs identified through exhaustive exploration under limited search budgets, it successfully constructs impressive Pareto fronts in the objective space (latency-resource utilization). This approach effectively satisfies design requirements while significantly reducing exploration overhead.

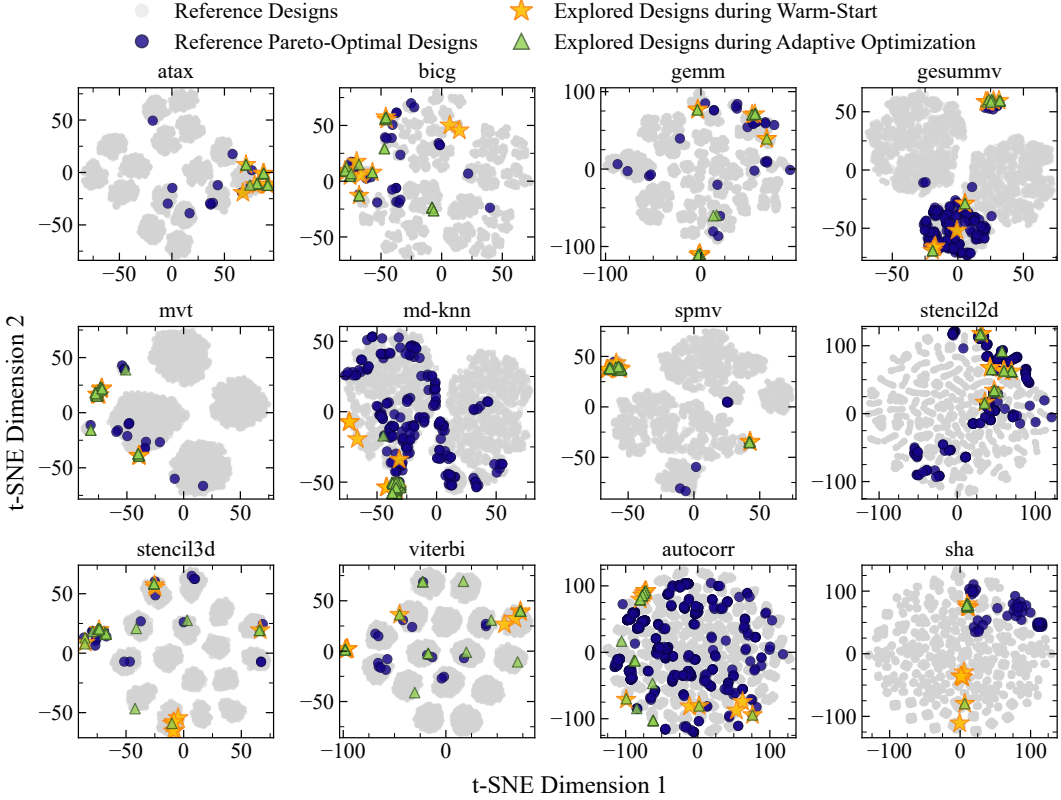


Figure 18: t-SNE visualization of reference Pareto-optimal and explored optimization directives in *Warm-Start* and *Adaptive Optimization* stages

D.5 Information of Assets

We provide all results of our experiments in our double-blind review repository, and we plan to upload our complete code for public after publication.

We present the information of assets as below:

1. Code

- HGBO-DSE [31]
 - License: MIT license.
 - URL: <https://github.com/hzkuang/HGBO-DSE>
- Lattice [21]
 - License: Available online.
 - URL: <http://www.inf.usi.ch/phd/ferretti/lattice-traversing-DSE.html>

2. Dataset

- PolyBench [90]
 - License: Ohio State University Software Distribution License.
 - URL: <http://polybench.sf.net>.
- CHStone [91]
 - License: Available online.
 - URL: <https://github.com/ferrandi/CHStone>
- MachSuite [92]
 - License: MachSuite BSD-3 license.
 - URL: <https://github.com/breagen/MachSuite>

E Limitations and Future Work

One limitation of our work is that LLMs cannot identify all ground-truth Pareto-optimal designs under finite search budgets, while exhaustive exploration remains impractical due to the vast design space. However, our experimental results demonstrate that iDSE significantly outperforms heuristic-based DSE methods, discovering Pareto fronts that, although potentially less diverse, are sufficiently impressive to satisfy multifaceted optimization preferences. Relaxing the maximum iteration limit would allow convergence toward a wider spectrum of Pareto-optimal designs at increased time cost. However, the effectiveness of LLMs may diminish with expanding exploration scales due to their limitations in handling long contexts. Our observations indicate that representative initial sampling designs generated by the LLM effectively enhance subsequent traditional evolutionary algorithms. Therefore, our method could be further improved by focusing on providing broader initial sampling designs combined with traditional DSE methods, thereby leveraging their established advantages in long-term hardware optimization.

Additionally, despite subsequent refinement, a modest number of low-quality directive configurations in the initial sampling still result in wasted evaluation time of the vendor HLS tool. We also observed that different general-purpose LLMs exhibit varying performance across benchmarks, with no single model consistently outperforming others, potentially complicating model selection for designers. A promising solution involves developing specialized models through targeted training, thus enhancing the scalability of the method, which we consider as an improvement direction for future work in iDSE. Furthermore, our iDSE framework can also serve as a data augmentation method for collecting high-quality datasets in DSE to drive future model training. Despite these limitations, we believe that iDSE represents pioneering work which provides valuable insights into the future of processor-level design space exploration, motivates efforts to apply generative AI to hardware optimization, and pushes the boundary of electronic design automation.